Mitochondrial division occurs concurrently with autophagosome formation but independently of Drp1 during mitophagy

Shun-ichi Yamashita,[1] Xiulian Jin,[1] Kentaro Furukawa,[1] Maho Hamasaki,[2] Akiko Nezu,[2] Hidenori Otera,[3] Tetsu Saigusa,[1] Tamotsu Yoshimori,[2] Yasuyoshi Sakai,[4] Katsuyoshi Mihara,[3] and Tomotake Kanki[1]

[1]Department of Cellular Physiology, Niigata University Graduate School of Medical and Dental Sciences, Niigata 951-8510, Japan
[2]Department of Genetics, Graduate School of Medicine, Osaka University, Osaka 565-0871, Japan
[3]Department of Molecular Biology, Graduate School of Medical Science, Kyushu University, Fukuoka 812-8582, Japan
[4]Division of Applied Life Sciences, Graduate School of Agriculture, Kyoto University, Kyoto 606-8502, Japan

Mitophagy is thought to play an important role in mitochondrial quality control. Mitochondrial division is believed to occur first, and autophagosome formation subsequently occurs to enwrap mitochondria as a process of mitophagy. However, there has not been any temporal analysis of mitochondrial division and autophagosome formation in mitophagy. Therefore, the relationships among these processes remain unclear. We show that the mitochondrial division factor Dnm1 in yeast or Drp1 in mammalian cells is dispensable for mitophagy. Autophagosome formation factors, such as FIP200, ATG14, and WIPIs, were essential for the mitochondrial division for mitophagy. Live-cell imaging showed that isolation membranes formed on the mitochondria. A small portion of the mitochondria then divided from parental mitochondria simultaneously with the extension of isolation membranes and autophagosome formation. These findings suggest the presence of a mitophagy process in which mitochondrial division for mitophagy is accomplished together with autophagosome formation.

Introduction

Macroautophagy (hereafter autophagy) is a catabolic process that nonselectively degrades cytoplasmic components and organelles. Upon induction of autophagy, double-membranous structures, called isolation membranes, emerge in the cytosol. The isolation membrane extends and sequesters cytoplasmic proteins and organelles, forming an autophagosome. The autophagosome then fuses with vacuoles in yeast or lysosomes in mammalian cells, and lysosomal hydrolases degrade the sequestered material (Nakatogawa et al., 2009). Mitochondrial autophagy, or mitophagy, is a process that selectively degrades mitochondria via autophagy (Lemasters, 2005). Recently, several studies have suggested that mitophagy contributes to mitochondrial quality control by eliminating excess or damaged mitochondria (Narendra et al., 2008; Twig et al., 2008).

Mitochondria are important organelles that produce most of the ATP required for cellular activities. Mitochondria move along with microtubules and change their size and morphology by division and fusion (Otera et al., 2013). When mitochondrial division is inhibited, unopposed fusion results in mitochondrial clustering or elongation. Conversely, when mitochondrial fusion is inhibited, unopposed division results in mitochondrial fragmentation (Detmer and Chan, 2007). Three GTPases are the core machineries for mitochondrial division and fusion. Dnm1 in yeast and Drp1 in mammals are dynamin-related proteins that mediate mitochondrial division. Recruitment of Dnm1/Drp1 on the mitochondrial division site is mediated by Fis1 in yeast and mitochondrial fission factor (Mff) 1, MiD49, and MiD51 in mammals (Detmer and Chan, 2007; Otera et al., 2013). Mitofusin (MFN; Fzo1 in yeast and Mfn1/Mfn2 in mammals) is a GTPase that is required for mitochondrial outer membrane fusion. Mgm1 in yeast and Opa1 in mammals are dynamin-related proteins that are required for mitochondrial inner membrane fusion.

The various sizes and shapes of mitochondria in cells are caused by mitochondrial division and fusion. Typical mitochondria show a short cylindrical or long tubular shape. The diameter of mitochondria is relatively constant in most cells (0.5–1.0 µm), whereas their length varies greatly (1–10 µm or more; Griparic and van der Bliek, 2001; Detmer and Chan, 2007). During mitophagy, autophagosomes completely enwrap mitochondria and then fuse with lysosomes/vacuoles. Therefore, the size of mitochondria should be smaller than autophagosomes.

Correspondence to Tomotake Kanki: kanki@med.niigata-u.ac.jp

Abbreviations used: CCCP, carbonyl cyanide m-chlorophenylhydrazone; CRISPR, clustered regularly interspaced short palindromic repeats; DFP, deferiprone; KO, knockout; MEF, mouse embryonic fibroblast; Mff, mitochondrial fission factor; MFN, mitofusin; WT, wild type.

The Rockefeller University Press $30.00
J. Cell Biol. Vol. 215 No. 5 649–665
https://doi.org/10.1083/jcb.201605093

In mammalian cells, the diameter of autophagosomes is usually 0.5–1.5 µm, whereas in yeast, it is 0.5–0.9 µm (Mizushima et al., 2002). This suggests that short, cylindrical-shaped mitochondria can be enwrapped immediately by autophagosomes, whereas long, tubular mitochondria should be severed to a suitable size before or simultaneously with autophagosome formation. Because dynamin-like Dnm1/Drp1-dependent mitochondrial division is only established with the severing of mitochondria, Dnm1/Drp1 might have an important role in mitophagy. Although accumulating evidence has suggested that Dnm1/Drp1 are required for mitophagy in yeast (Kanki et al., 2009b; Abeliovich et al., 2013; Mao et al., 2013) and in mammalian cells (Tanaka et al., 2010; Rambold et al., 2011; Kageyama et al., 2014; Ikeda et al., 2015), a limited number of studies have also reported that Dnm1/Drp1 are not required for mitophagy in yeast (Mendl et al., 2011; Bernhardt et al., 2015) and in mammalian cells (Song et al., 2015). Therefore, whether Dnm1/Drp1-mediated mitochondrial division has an important role in mitophagy remains controversial.

Our study shows that mitochondrial division occurs after the formation of isolation membranes and in cooperation with the extension of isolation membranes and is independent of Dnm1/Drp1-mediated mitochondrial division. This mitophagy process is completely different from the widely believed model that mitochondrial division occurs first and then autophagosomes enwrap the divided mitochondria.

Results

Dnm1-independent mitochondrial division occurs during mitophagy in yeast

To monitor mitophagy in yeast, the method of tagging mitochondrial proteins with GFP is widely used (Kanki et al., 2009a; Okamoto et al., 2009). We tagged GFP at the C terminus of the mitochondrial matrix protein Idh1. When mitophagy is induced, mitochondria are delivered into vacuoles and Idh1-GFP is degraded. However, GFP alone is relatively stable within vacuoles and is released as an intact protein. The level of mitophagy can thus be semiquantitatively monitored by measuring the amount of GFP processed from Idh1-GFP by immunoblotting. When mitophagy was induced by nitrogen starvation or culturing cells to the post-log phase in wild-type (WT) cells, free GFP processed from Idh1-GFP was observed (Fig. 1, A and C). In mitophagy-defective *atg11Δ* cells (Kanki and Klionsky, 2008) cultured under both mitophagy induction conditions, free GFP was not observed (Fig. 1, A and C).

To determine whether mitochondrial division is required for mitophagy, we first examined mitophagy in mitochondrial division–deficient yeast (*Saccharomyces cerevisiae*) mutants. As shown in Fig. S1 A, when *DNM1*, *FIS1*, or *CAF4*/*MDV1* (all mitochondrial division factors) was deleted, mitochondrial division was inhibited, and mitochondria showed interconnected tubular or net forms caused by ongoing mitochondrial fusion. Morphological changes of mitochondria could be observed more obviously when mitochondria were visualized by the expression of GFP-tagged mitochondrial outer membrane protein Om45 (Om45-GFP; Fig. S1 A). In the mitochondrial fusion factor *FZO1*-deleted strain, mitochondrial fusion was inhibited, and mitochondria showed a fragmented form (Fig. S1 A). In *dnm1Δ* cells in which mitophagy was induced by nitrogen starvation, mitophagy induction was slightly decreased but still occurred at a substantial level (Fig. 1 A). Although Dnm1 and Fis1 work cooperatively in mitochondrial division and deletion of either protein showed the same mitochondrial morphology, mitophagy was lower in *fis1Δ* than in *dnm1Δ* cells (Fig. 1 A). However, when cells were starved for longer periods, degradation of Idh1-GFP reached the same level in *dnm1Δ* and *fis1Δ* cells as that in WT cells, whereas degradation remained inhibited in mitophagy-defective *atg11Δ* cells (Fig. 1 B). This finding suggests that mitophagy occurs but is delayed in *dnm1Δ* and *fis1Δ* cells. Similarly, mitophagy induced at the post-log phase was not affected in *dnm1Δ* or *fis1Δ* cells compared with WT cells (Fig. 1 C).

We next tested whether mitochondrial division is required for mitophagy in another species of budding yeast, *Pichia pastoris* (Sakai et al., 1998). Similar to *S. cerevisiae*, we found that mitophagy was only partially inhibited in *P. pastoris dnm1Δ* cells (Fig. 1 D). Based on our results, we conclude that Dnm1 is not an essential factor for mitophagy, although its deletion may affect the efficiency of mitophagy or delay the induction of mitophagy.

Dnm1 is the only identified molecular motor for mitochondrial division. Therefore, the mechanism underlying how enlarged mitochondria are enwrapped by autophagosomes and delivered into vacuoles in *dnm1Δ* cells remains elusive. To address this issue, we examined autophagosomes and autophagic bodies containing mitochondria as a cargo, termed mitophagosomes and mitophagic bodies, respectively, by fluorescence microscopy and EM. Ypt7 is a Rab GTPase family protein that is required for fusion between autophagosomes and vacuoles (Kirisako et al., 1999). Therefore, mitophagosomes should accumulate within the cytoplasm of *ypt7Δ* cells after induction of mitophagy. Although most mitochondria were localized adjacent to the plasma membrane in *ypt7Δ* cells, some punctate mitochondria were localized near the center of the cells only after the induction of mitophagy (Fig. 1 E and Fig. S1, B and C). These punctate mitochondria that appear near the center of cells colocalized with the autophagosome marker RFP-Atg8 (Fig. S1 D). In *atg11Δ*/*ypt7Δ* cells, which cannot induce mitophagy, all of the mitochondria were localized adjacent to the plasma membrane, and punctate mitochondria were not observed near the center of cells, even under the condition of mitophagy (Fig. 1 E). These findings suggest that the punctate mitochondria that appear after the induction of mitophagy near the center of cells in *ypt7Δ* cells are mitophagosomes. In *dnm1Δ*/*ypt7Δ* cells, besides tubular mitochondria localized adjacent to the plasma membrane, small punctate mitochondria were observed near the center of cells (Fig. 1 E and Fig. S1, C and D). This finding suggests that mitophagosomes containing small punctate mitochondria also form in Dnm1-deficient cells.

In *pep4Δ* cells, which lack one of the main vacuolar hydrolases, mitophagic bodies are not degraded and accumulated in vacuoles (Takeshige et al., 1992). EM showed that the diameters of mitochondria in mitophagic bodies were ∼600 nm or less in *pep4Δ* cells (Figs. 1 F and S1 E). In *pep4Δ*/*dnm1Δ* cells, similar numbers of mitophagic bodies accumulated in vacuoles under the condition of mitophagy (Figs. 1 F and S1 F). Notably, mitochondria in mitophagic bodies in *pep4Δ*/*dnm1Δ* cells also showed a diameter of ∼600 nm or less. However, almost all of the cytosolic mitochondria were clustered spherical, long tubular, or net forms, and none had a small spherical shape (Figs. 1 F and S1 F). These findings strongly suggest that Dnm1-independent division of mitochondria occurs during mitophagy and that this division always produces small spherical mitochondria (∼600 nm in diameter) from a large parental mitochondrial mass.

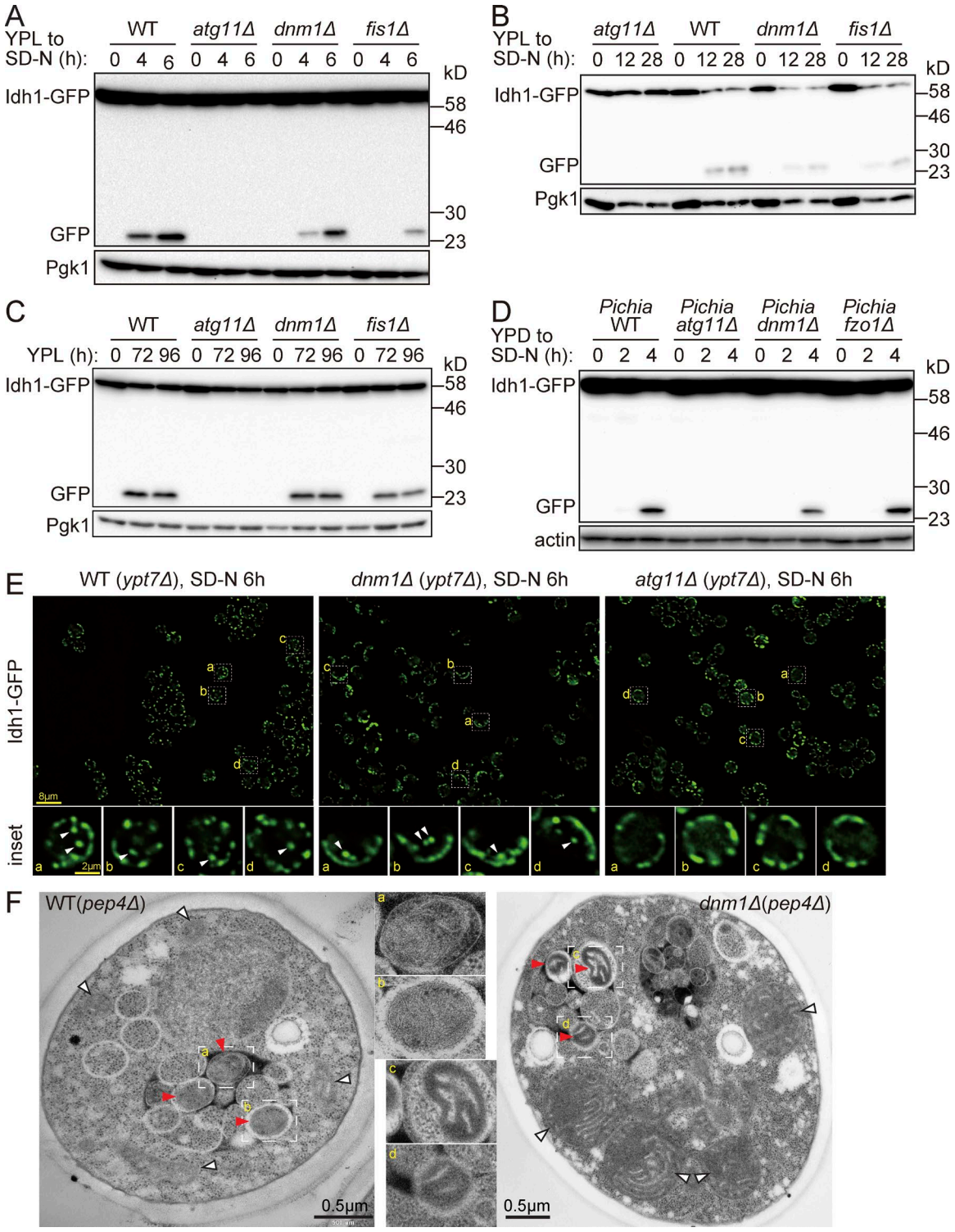

Figure 1. **Dnm1-independent mitochondrial division occurs during mitophagy in yeast.** (A–C) WT, *atg11Δ*, *dnm1Δ*, and *fis1Δ* cells expressing Idh1-GFP were cultured in YPL medium until the mid-log growth phase. Cells were then shifted to SD-N medium for 0, 4, and 6 h (A) or 12 and 48 h (B), or cells were cultured in YPL up to 96 h (C). Reduction of Idh1-GFP and processed GFP was monitored as a result of mitophagy by immunoblotting with anti-GFP and anti-Pgk1 (loading control) antibodies. (D) WT, *atg11Δ*, *dnm1Δ*, and *fis1Δ P. pastoris* cells expressing Idh1-GFP were cultured in YPD medium until the mid-log growth phase and then were transferred to SD-N medium for 0, 2, and 4 h. Processing of Idh1-GFP was observed as a result of mitophagy by immunoblotting with anti-GFP and anti–β-actin (loading control) antibodies. (E) The indicated cells expressing Idh1-GFP were cultured in YPL medium until the mid-log growth phase and then shifted to SD-N medium for 6 h. GFP signals were observed by fluorescence microscopy. Arrowheads indicate mitochondria presumed to be within the mitophagosome. (F) The indicated cells were cultured in YPL medium until the mid-log growth phase and then shifted to SD-N medium for 6 h. Cells were collected and processed for EM using the high-pressure freezing method and then were observed with a transmission electron microscope. White arrowheads indicate cytosolic mitochondria, and red arrowheads indicate mitophagic bodies.

Drp1 is dispensable for hypoxia- or deferiprone (DFP)-induced mitophagy in mammalian cells

We next examined mitophagy in mitochondrial division–deficient mammalian cells. To monitor mitophagy, we used the pH-sensitive fluorescent protein Keima (Katayama et al., 2011; Hirota et al., 2015; Lazarou et al., 2015). When Keima is present in a neutral environment, such as the mitochondrial matrix, this fluorescent protein is excited by 440-nm light, but not by 590-nm light. However, when Keima is present in acidic conditions, such as in autolysosomes, this fluorescent protein is excited by 590-nm light, but not by 440-nm light. We expressed mitochondrial matrix–localizing Keima (mito-Keima) in HeLa cells, SH-SY5Y cells, and mouse embryonic fibroblasts (MEFs). We induced mitophagy under hypoxic conditions or by treatment with DFP, an iron-chelating drug (Liu et al., 2012; Allen et al., 2013). Before the induction of mitophagy, mito-Keima was localized within the mitochondrial matrix, excited by 440-nm light, and showed tubular mitochondria-like shapes (Fig. 2, A and G). After induction of mitophagy, some portions of mitochondria were delivered into lysosomes, and then mito-Keima was released to the lysosomal lumen. Excitation of the lysosomal mito-Keima was changed to 590-nm light, and this was observed as punctate structures (Fig. 2, A and G). These punctate structures colocalized with the lysosome marker LAMP1-EGFP (Fig. S2 A) and were suppressed by knockdown of the autophagy-related gene *FIP200* (Fig. 2, A–C) or *Beclin-1* (Hirota et al., 2015).

To examine whether Drp1, a mammalian homologue of Dnm1, has a role in mitophagy, we generated Drp1 knockout (KO) HeLa cells using the clustered regularly interspaced short palindromic repeats (CRISPR)–Cas9 method (Fig. 2 D; Otera et al., 2016) and monitored mitophagy. Although mitochondria were clustered with extended tubules in Drp1 KO cells, mitophagy induced by hypoxia or DFP was at a comparable level with that in WT cells (Fig. 2, F and G). Quantification of the number of mitophagic puncta (punctate structures observed by 590-nm excitation light) showed that mitophagy was slightly decreased in Drp1 KO cells compared with WT cells (Fig. 2 E). Similar results were observed in Drp1$^{-/-}$ MEFs (Ishihara et al., 2009) or Drp1 knockdown HeLa and SH-SY5Y cells (Fig. 2, A–C; and Fig. 3, A–C). KO of the other mitochondrial division factors, such as Mff, Fis1, or MiD49/MiD51, also marginally affected hypoxia or DFP-induced mitophagy (Fig. 3, D and E). To further confirm that mitophagy can be induced in Drp1 KO cells, we used mitochondria-targeted mCherry-EGFP (mito-mCherry–EGFP) to observe mitophagy (Allen et al., 2013). Mito-mCherry–EGFP localizes within the mitochondrial matrix. When mitochondria were delivered into lysosomes by mitophagy, EGFP was degraded earlier than mCherry, or EGFP fluorescent signal was easily quenched within the lysosome. Thus, the lysosomal punctate mCherry signal without EGFP was observed as evidence of mitophagy. As shown in Fig. S2 (B–D), mitophagy was induced to almost similar levels in both WT and Drp1 KO cells. To further obtain supportive evidence of mitophagy, we examined the reduction of mitochondrial proteins Tom20 and Tim23 under mitophagic conditions by immunoblotting. As shown in Fig. S2 E, these proteins decreased to similar levels in WT and Drp1 KO cells after mitophagy induction. Based on these findings, we conclude that, similar to yeast, Drp1 is not an essential factor for hypoxia or DFP-induced mitophagy, although it affects the efficiency of mitophagy.

Parkin, an E3 ubiquitin ligase, accumulates on depolarized mitochondria and ubiquitinates many mitochondrial outer membrane proteins. These ubiquitinated mitochondria are eventually degraded by mitophagy (Narendra et al., 2008). Parkin-mediated mitophagy has been intensively studied, and Tanaka et al. (2010) have suggested that Drp1 plays an important role in this type of mitophagy. Thus, we next tested whether Parkin-mediated mitophagy is suppressed in our Drp1 KO cells. We exogenously expressed Parkin together with NLS-tagged GFP in mito-Keima–expressing WT and Drp1 KO HeLa cells. Cells were treated with carbonyl cyanide m-chlorophenylhydrazone (CCCP) to induce mitophagy. We noticed that Parkin-expressing Drp1 KO cells died earlier than WT cells after CCCP treatment (half of the cells died within 12 h of CCCP treatment). Thus, we observed mitophagy after CCCP treatment for 6 h, although this time course is quite short compared with most previous publications (Narendra et al., 2008; Geisler et al., 2010). Interestingly, substantial mitophagic signals were observed in both WT and Drp1 KO cells induced for Parkin-mediated mitophagy, and the mitophagy was only slightly decreased in Drp1 KO cells compared with WT cells (Fig. S3, A and B).

Fragmentation of mitochondria does not accelerate mitophagy

Because the size of autophagosomes is limited, mitochondria smaller than autophagosomes might be easily enwrapped by autophagosomes. Therefore, we tested whether mitophagy is increased in cells with hyperfragmented mitochondria. To induce mitochondrial fragmentation, we knocked down the mitochondrial fusion factors Mfn1 and Mfn2 in WT and Drp1 KO cells. In Mfn1 and Mfn2 double knockdown cells, mitochondria were fragmented and smaller in size than control siRNA-treated cells, but the amount of mitophagy induced by hypoxia and DFP treatment did not dramatically change (Fig. 4). Overexpression of the mitochondrial division factor Mff also induces mitochondrial fragmentation (Otera et al., 2010). Therefore, we next overexpressed Mff in WT cells and monitored mitophagy. Although overexpression of Mff induced mitochondrial fragmentation, it suppressed mitophagy (Fig. S3, C and D). Currently, we cannot explain the mechanism by which overexpression of Mff suppresses mitophagy. However, based on our findings, we conclude that fragmentation of mitochondria does not accelerate mitophagy.

Drp1-independent mitochondrial fragmentation appears during mitophagy in mammalian cells

In Drp1 KO cells, whether a typically sized autophagosome enwraps small punctate mitochondria or an untypically large autophagosome enwraps large clustered or long tubular mitochondria during mitophagy is unknown. To examine how autophagosomes enwrap mitochondria, we used bafilomycin A1 to inhibit fusion of autophagosomes with lysosomes (Klionsky et al., 2008) under a mitophagy condition. Without bafilomycin A1 treatment, mitophagic puncta, which were excited by 590-nm light, appeared in WT and Drp1 KO HeLa cells expressing mito-Keima upon hypoxia and DFP treatment (Fig. 5, A and B). When cells were treated with bafilomycin A1, mitophagy was almost completely inhibited, and small punctate mitochondria, which were excited by 440-nm light, were observed upon mitophagy (Fig. 5 A). Notably, in

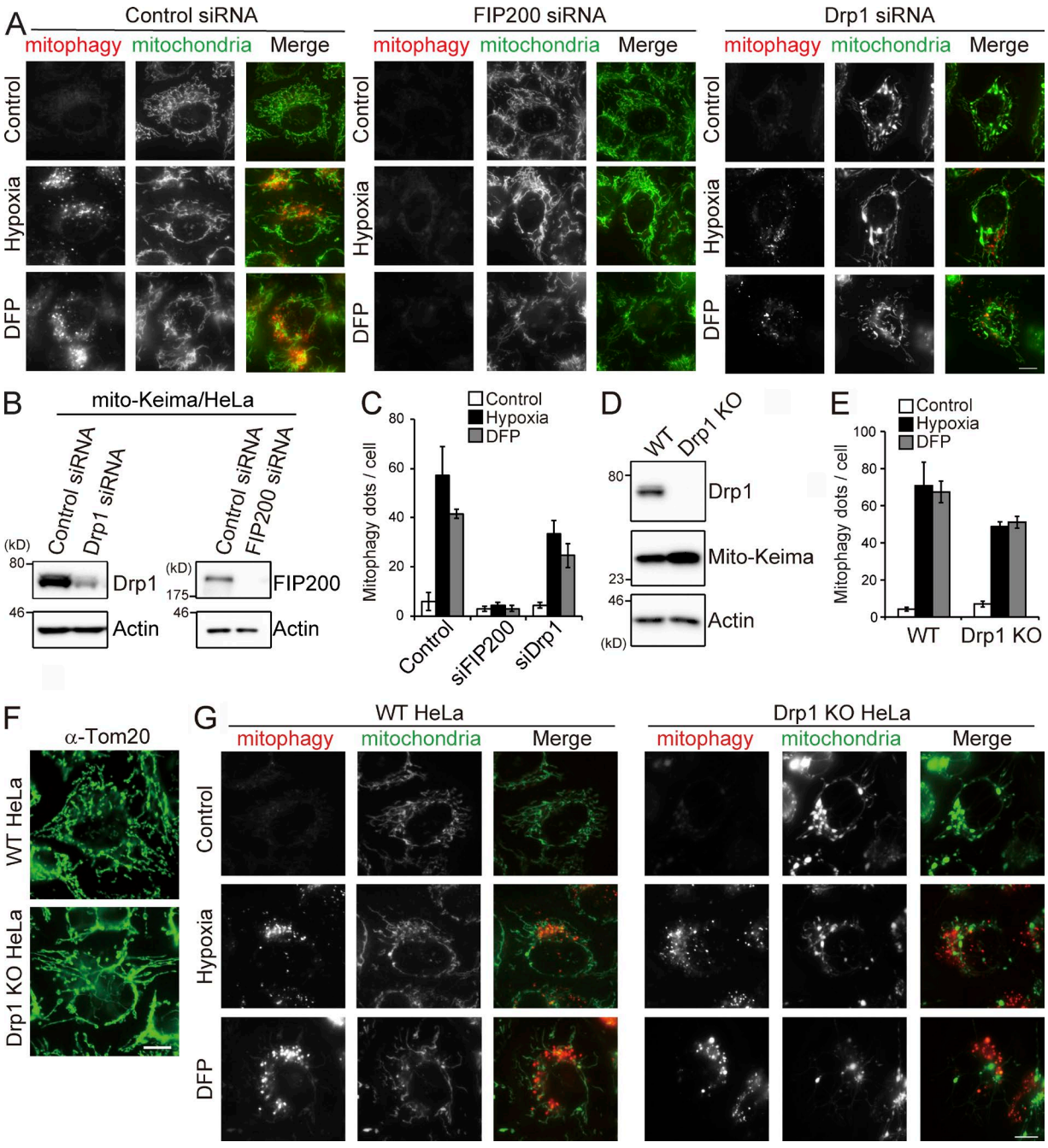

Figure 2. **Drp1 is not an essential factor for hypoxia and DFP-induced mitophagy in HeLa cells.** (A–C) HeLa cells stably expressing mito-Keima were transfected with the indicated siRNAs and cultured under hypoxic conditions or normal conditions in the presence of 1 mM DFP for 24 h. Cells were then analyzed by fluorescence microscopy with two excitation filters. Mito-Keima is excited by 590-nm light in lysosomes, indicating mitophagy (mitophagy dots; red), and excited by 440-nm light in the mitochondrial matrix, indicating mitochondria (green; A). The cells were lysed and analyzed by immunoblotting with anti-FIP200, anti-Drp1, and anti-actin antibodies (B). Mitophagy dots were calculated from at least 50 cells under control, hypoxic, and DFP treatment conditions as shown in A. Data are shown as the mean ± SD of three independent experiments (C). (D–G) WT and Drp1 KO HeLa cells stably expressing mito-Keima were lysed and analyzed by immunoblotting with anti-Drp1, anti-Keima, and anti-actin antibodies (D). (E) Mitophagy dots shown in G were calculated as in C. (F) WT and Drp1 KO HeLa cells were examined by immunofluorescence microscopy with anti-Tom20 antibody. (G) WT and Drp1 KO HeLa cells were cultured under DFP-induced mitophagy conditions and analyzed by fluorescence microscopy as in A. Data are shown as the mean ± SD of three independent experiments. Bars, 10 µm.

addition to tubular or clustered mitochondria, small punctate mitochondria were observed in Drp1 KO cells (Fig. 5 B). Syntaxin 17 (Stx17) is required for fusing autophagosomes with lysosomes (Itakura et al., 2012). To confirm the observations with bafilomycin A1, we inhibited fusion of autophagosomes with lysosomes by knockdown of Stx17. When Stx17 was knocked down, mitochondrial morphology was affected (Fig. S4), as reported previously (Arasaki et al., 2015). As shown in Fig. S4 (A and B), mitophagy induced by both hypoxia and DFP was suppressed as a result of autophagosome and lysosome fusion defects. Under these conditions, small punctate mitochondria were observed within the cytosol, even in Drp1

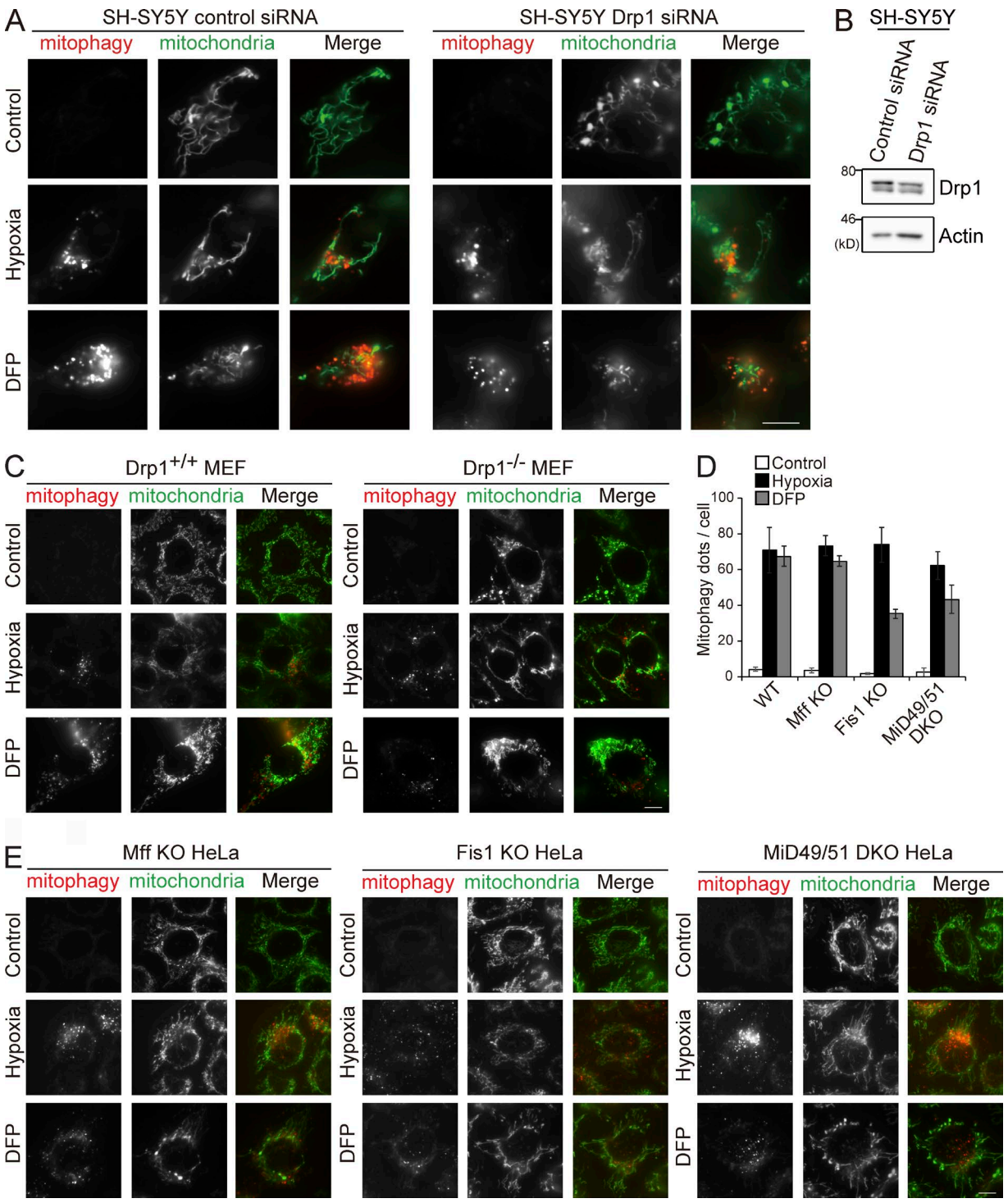

Figure 3. **Drp1 is not an essential factor for hypoxia or DFP-induced mitophagy in several types of mammalian cells.** (A) SH-SY5Y cells stably expressing mito-Keima were transfected with control and Drp1 siRNA, cultured under hypoxia or DFP-induced mitophagy conditions, and analyzed by fluorescence microscopy, as in Fig. 2 A. (B) Cells transfected with control and Drp1 siRNA were lysed and analyzed by immunoblotting with anti-Drp1 and anti-actin antibodies. (C) WT and Drp1$^{-/-}$ MEFs stably expressing mito-Keima were cultured under hypoxia or DFP-induced mitophagy conditions and monitored as in Fig. 2 A. (D) Mitophagy dots shown in E (Mff KO, Fis1 KO, and Mid49/51 KO) were calculated as in Fig. 2 C. (E) Mff KO, Fis1 KO, and MiD49/51 double KO HeLa cells stably expressing mito-Keima were cultured under hypoxia or DFP-induced mitophagy conditions and monitored as in Fig. 2 A. This experiment was performed together with the experiment shown in Fig. 2 G. Data are shown as the mean ± SD of three independent experiments. Bars, 10 µm.

KO cells (Fig. S4 A). These punctate mitochondria were rarely observed without inhibition of autophagosome and lysosome fusion in Drp1 KO cells, suggesting that they were mitochondria within autophagosomes.

To confirm whether these punctate mitochondria are enwrapped by autophagosomes, we performed immunofluorescence microscopy with antibodies against the mitochondrial outer membrane protein Tom20 and the autophagosome

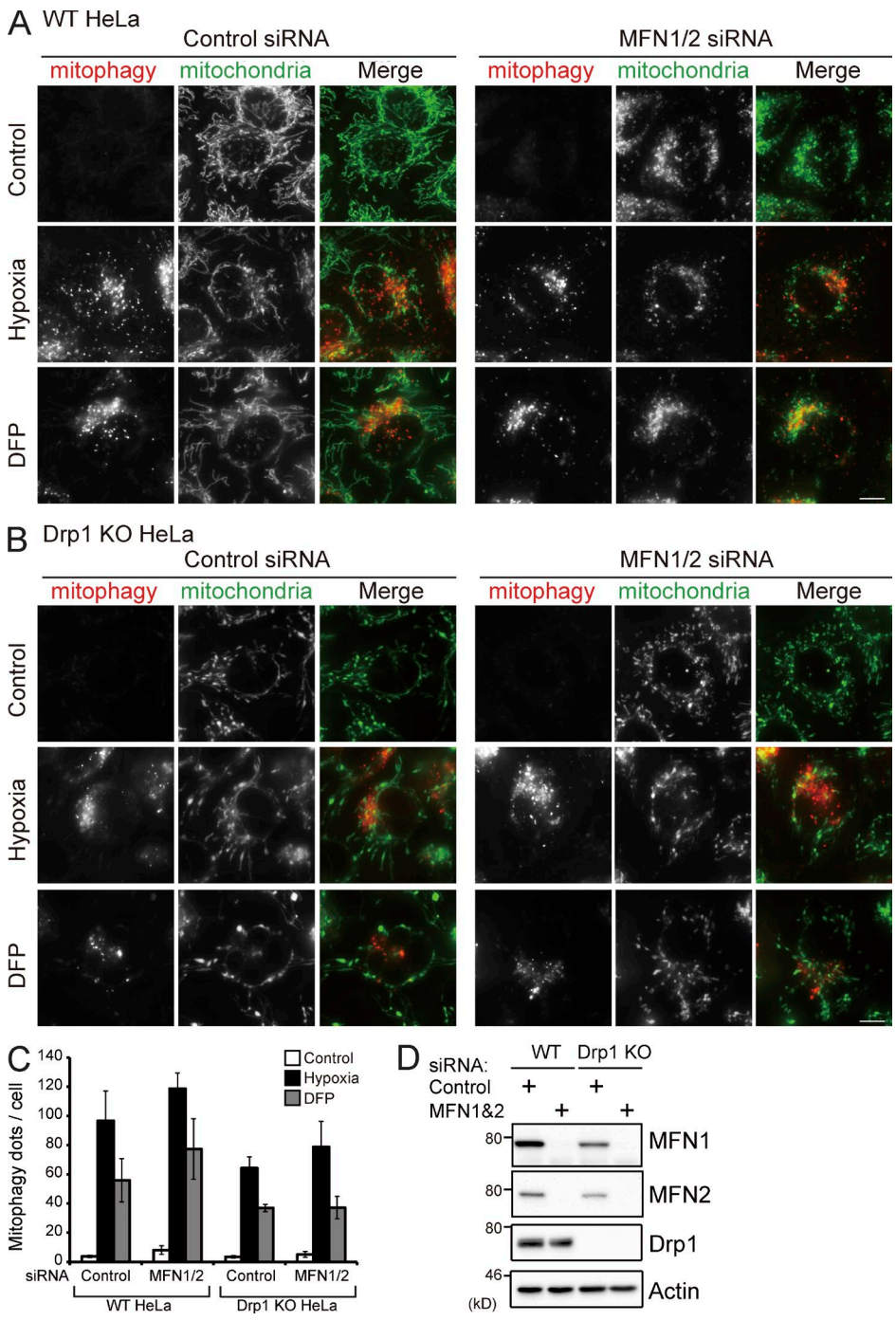

Figure 4. **Fragmentation of mitochondria does not accelerate mitophagy.** (A and B) WT (A) and Drp1 KO (B) cells stably expressing mito-Keima were transfected with control or MFN1/2 siRNAs and cultured under mitophagy conditions as in Fig. 2 A. Bars, 10 µm. (C) Mitophagy dots shown in A and B were calculated as in Fig. 2 C. Data are shown as the mean ± SD of three independent experiments. (D) Cells transfected with control and MFN1/2 siRNAs were lysed and analyzed by immunoblotting with anti-MFN1, anti-MFN2, anti-Drp1, and anti-actin antibodies.

marker protein LC3. Consistent with results shown in Fig. 5, small punctate mitochondria appeared only after the induction of mitophagy, and the majority of these punctate mitochondria, but not tubular mitochondria, were colocalized with LC3 in both WT and Drp1 KO cells (Fig. 6 A). Furthermore, small mitochondria enwrapped by double membrane were observed by EM in WT and Drp1 KO cells upon mitophagy conditions (Fig. 6 B). Collectively, these findings suggest that small punctate mitochondria are enwrapped by autophagosomes.

In the vast majority of cases, isolation membrane nucleation occurs on tubular mitochondria and then a small portion of mitochondria is divided from parental mitochondria concomitant with autophagosome formation

We next decided to examine the process of how isolation membranes are formed and enwrap mitochondria. We visualized isolation membranes and mitochondria by expressing EGFP-LC3B and mitochondria-targeted mCherry (mito-mCherry), respectively, and performed time-lapse imaging after DFP treatment

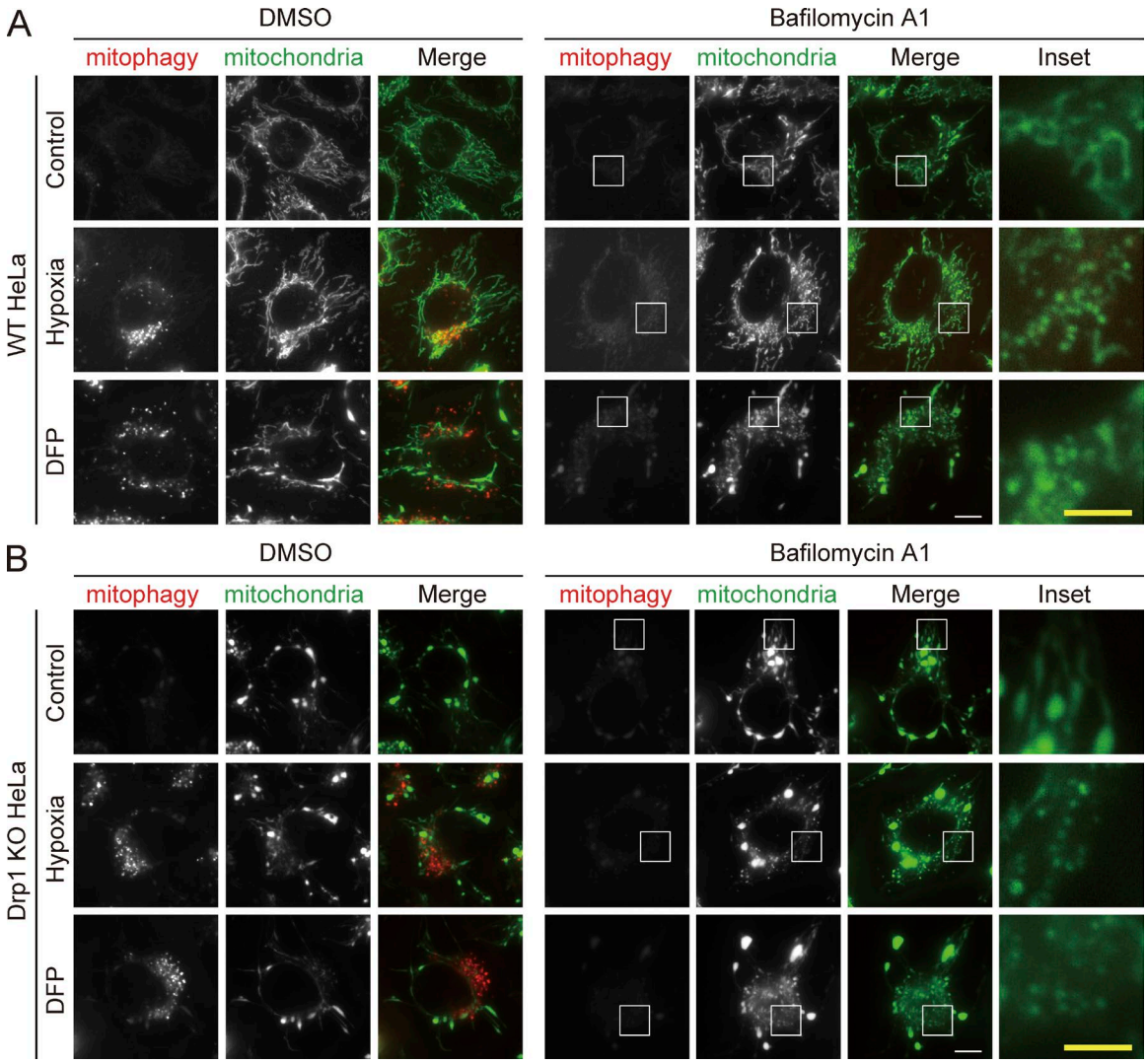

Figure 5. **Drp1-independent mitochondrial fragmentation appears under the condition of mitophagy in HeLa cells.** (A and B) WT (A) and Drp1 KO (B) cells expressing mito-Keima were cultured under the condition of mitophagy as in Fig. 2 A in the presence of DMSO (left columns) and bafilomycin A1 (right columns). Bars: (merged views) 10 µm; (insets) 5 µm.

for 12 h. Typical images of mitophagy in WT cells showed that a signal of EGFP-LC3B emerged on tubular mitochondria, and its signal intensity gradually increased as mitophagy progressed. This finding suggested that nucleation of isolation membranes and their extension occurs on the surface of mitochondria (Fig. 7, A and B). This is further supported by the colocalization of EGFP-LC3B with BFP-WIPI1, which is known to accumulate on isolation membranes (Fig. S4 C; Proikas-Cezanne et al., 2007). After an increase in EGFP-LC3B intensity, in most cases, EGFP-LC3 colocalized with a small portion of mitochondria that had budded from tubular mitochondria and then divided, forming punctate mitochondria (Fig. 7 A). Occasionally, if an isolation membrane formed at the end of tubular mitochondria, a small portion of mitochondria divided without bud formation (Fig. 7 B). Finally, the punctate mitochondria that colocalized with EGFP-LC3B were completely released from parental mitochondria. In Drp1 KO cells, similar mitochondrial division was observed (Fig. 7, C and D). Under the condition of mitophagy, EGFP-LC3B signals appeared, and their intensity increased on the surface of clustered mitochondria in most cases. A small portion of mitochondria budded and divided from parental mitochondria after an increase in EGFP-LC3B intensity and formed small punctate mitochondria that colocalized with EGFP-LC3B (Fig. 7, C and D). These findings suggest that mitochondrial division resulting in punctate mitochondria under the condition of mitophagy occurs simultaneously with autophagosome formation in a Drp1-independent manner.

To confirm that Drp1 is not related to mitochondrial division during mitophagy, we expressed BFP-Drp1, EGFP-LC3B, and mito-mCherry in WT cells and performed time-lapse imaging after mitophagy induction. As previously reported (Smirnova et al., 2001), BFP-Drp1 localized on mitochondria, and the mitochondria were divided at the site of Drp1 (Fig. 8 A, white arrows). However, EGFP-LC3B was not localized at this site, and punctate mitochondria were not formed. We observed >50 cases of mitophagosome formation accompanying mitochondrial division; however, none of the sites of mitochondrial division colocalized with BFP-Drp1, as shown in Fig. 8 A (yellow arrows), suggesting that mitochondrial division at a mitophagosome formation site occurs independently of Drp1.

Next, we took time-lapse imaging of >150 EGFP-LC3B signals that emerged on mitochondria and observed their

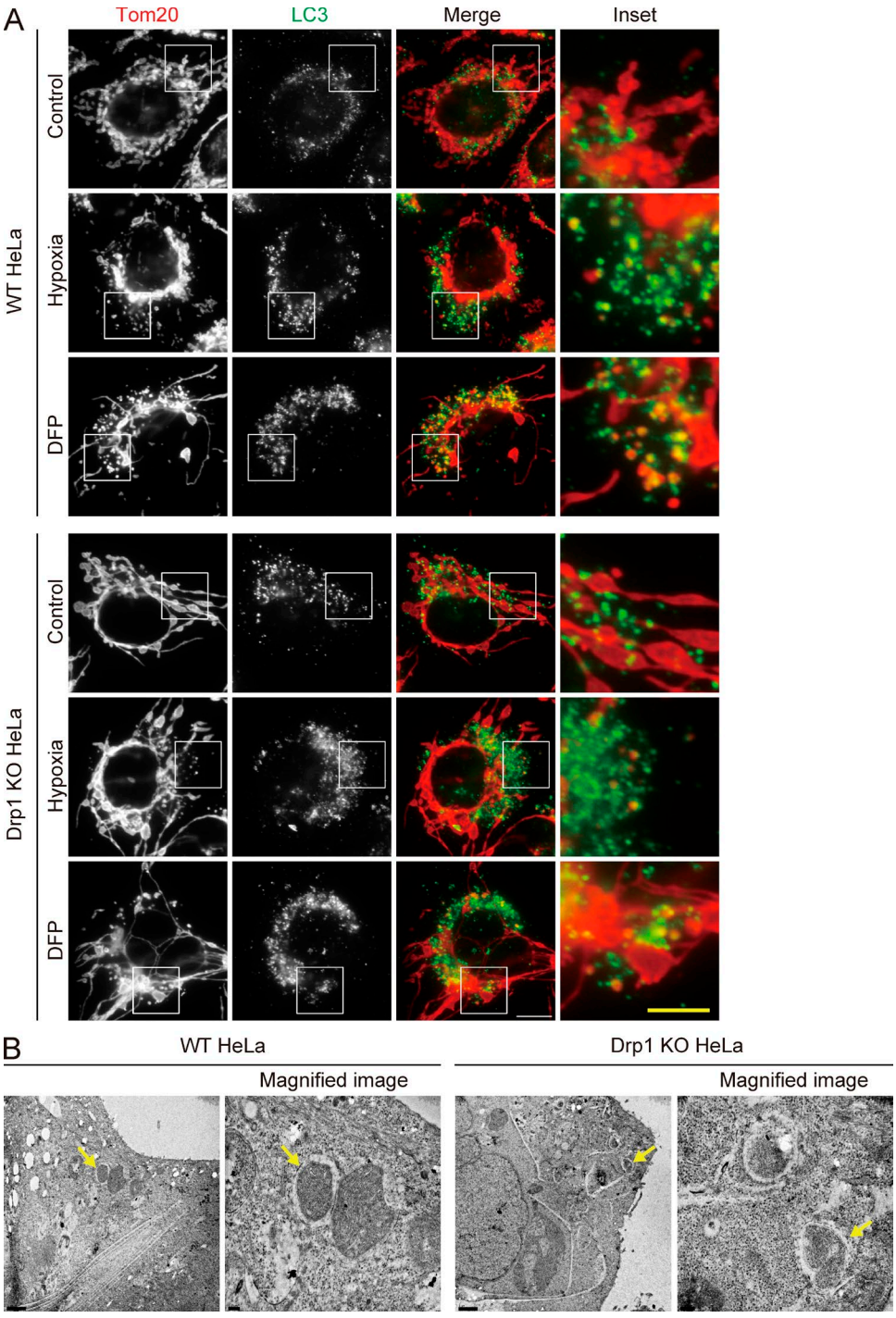

Figure 6. **Small mitochondrial puncta are enwrapped by autophagosomes upon induction of mitophagy.** (A) WT and Drp1 KO HeLa cells were cultured under normal and mitophagy conditions as in Fig. 2 A. The cells were treated with 100 nM bafilomycin A1 from 12 h after shifting to mitophagy conditions and cultured for an additional 12 h. The cells were examined by immunofluorescence microscopy with anti-Tom20 (red) and anti-LC3 (green). Bars: (merged views) 10 µm; (insets) 5 µm. (B) Electron micrographs of WT and Drp1 KO HeLa cells upon induction of mitophagy in the presence of 100 nM bafilomycin A1. Yellow arrows indicate autophagosomes, including small mitochondria. Bars: (main images) 1 µm; (magnified images) 0.2 µm.

destination (Fig. 8 B). In both WT and Drp1 KO cells, approximately half of the EGFP-LC3B signals became mitophagosomes (48% in WT and 50% in Drp1 KO cells), and the other half became autophagosomes without containing mitochondria, suggesting that the autophagosome is also formed on or near mitochondria (Hamasaki et al., 2013). The vast majority of mitophagosomes were formed on the tubular or clustered mitochondria (83% in WT and 98% in Drp1 KO cells). Notably, in all cases of mitophagosome formation on tubular or clustered mitochondria, mitochondrial division occurred simultaneously with mitophagosome formation, as shown in Fig. 7. Collectively, these findings suggest that the vast majority of mitochondrial division events for mitophagy occurred concomitantly with mitophagosome formation and in a Drp1-independent manner.

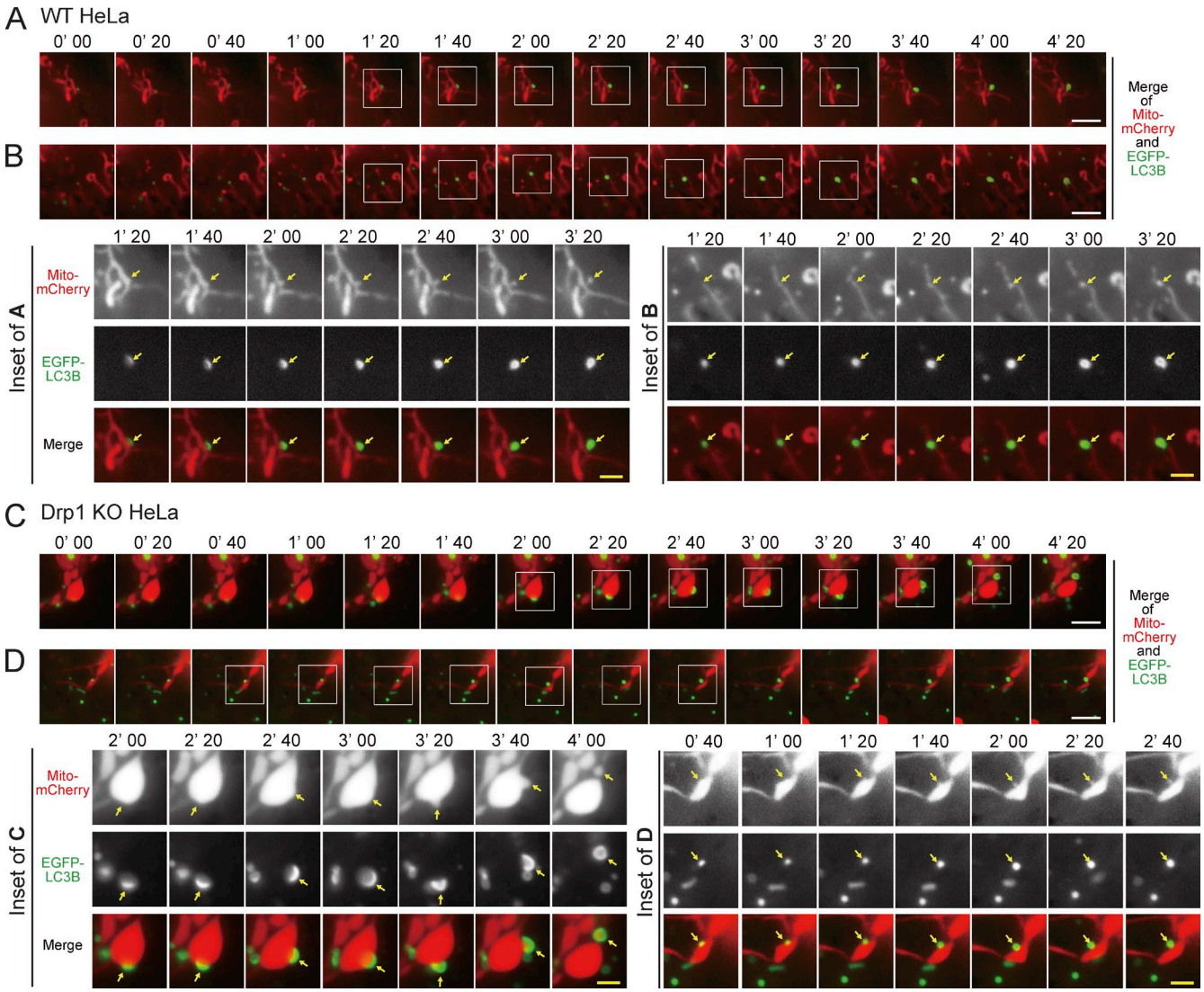

Figure 7. **Isolation membrane nucleation occurs on tubular mitochondria, and then a small portion of mitochondria is divided from parental mitochondria after autophagosome formation.** (A and B) Time-lapse images of WT cells coexpressing mito-mCherry and EGFP-LC3B under DFP treatment conditions. The cells were analyzed from 12 h after shifting to medium containing 1 mM DFP. Insets of A and B were divided into images of mito-mCherry and EGFP-LC3B. Isolation membrane and autophagosome formation sights are indicated by yellow arrows. (C and D) Time-lapse images of Drp1 KO cells as in A and B. Bars: (main images) 10 µm; (insets) 5 µm.

Finally, we measured the duration between isolation membrane emergence on the mitochondria and completion of mitophagosome formation in WT and Drp1 KO cells. We found that Drp1 KO cells needed more time to form mitophagosomes compared with WT cells (Fig. 8 C).

Isolation membrane formation and extension are required for mitochondrial division upon induction of mitophagy

Mitochondrial division is likely to occur together with autophagosome formation (Fig. 7). Therefore, we next tested whether autophagosome formation machinery is involved in mitochondrial division upon induction of mitophagy.

Autophagy-related protein complexes function in different steps of autophagosome formation (Levine et al., 2011; Nixon, 2013). After induction of autophagy, the ULK1 complex (ULK1, ATG13, FIP200, and ATG101) is first recruited to the autophagosome formation site. The class III phosphatidylinositol-3-OH kinase complex (VPS34, Beclin-1, Atg14, and Vps15) is then recruited to the site and produces phosphatidylinositol-3-phosphate. These complexes are essential for the formation of isolation membranes. Downstream of these complexes, the phosphatidylinositol-3-phosphate effecter proteins, comprised of the double FYVE–containing protein 1 (DFCP1) and the WD repeat domain phosphoinositide-interacting (WIPI) family–Atg2 complex, are required for the extension of isolation membranes. Finally, the extended membrane is sealed to form mature autophagosomes. Two ubiquitin-like conjugation systems (the Atg12–Atg5 conjugation system [Atg12, Atg7, Atg10, Atg5, and Atg16] and the LC3 conjugation system [Atg4, Atg7, and Atg3]) are thought to be related to the sealing of autophagosomes (Sou et al., 2008; Kishi-Itakura et al., 2014), although some of them are not essential for mitophagy (Fig. S5 A). Therefore, we knocked down the genes *FIP200*, *ATG14*, *WIPI* (*WIPI1*, *WIPI2*, *WDR45L*, and *WDR45*), *ATG5*, and *ATG3* to arrest autophagosome formation at each step and

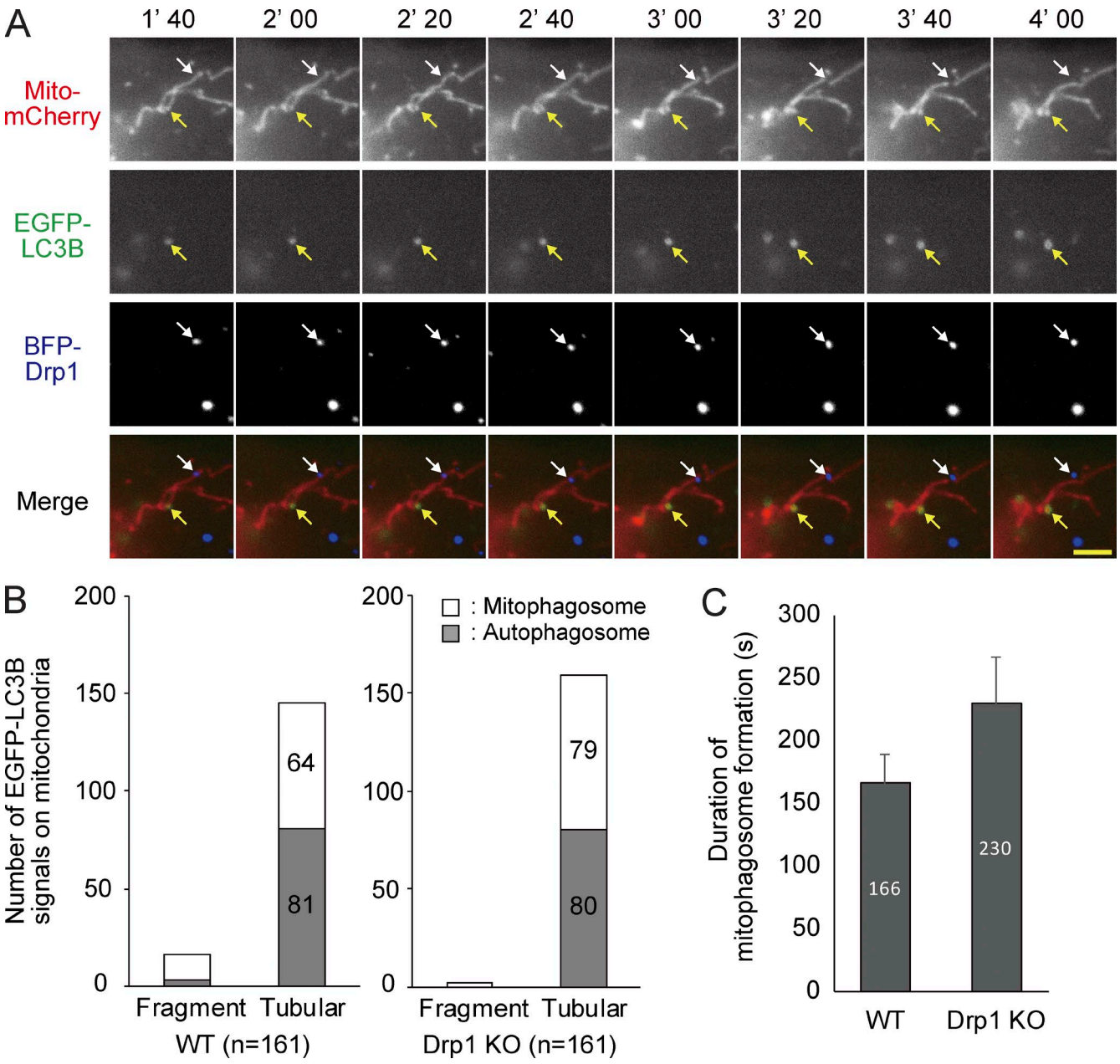

Figure 8. **Quantitative analysis of time-lapse imaging of mitophagosome formation and mitochondrial division.** (A) Time-lapse images of WT cells coexpressing mito-mCherry, EGFP-LC3B, and BFP-Drp1 under DFP treatment conditions. The cells were analyzed from 12 h after shifting to medium containing 1 mM DFP. The sites of Drp1-dependent mitochondrial fission and mitophagosome formation are indicated by white and yellow arrows, respectively. Bar, 5 µm. (B) Time-lapse imaging data of WT and Drp1 KO cells as shown in Fig. 7 were collected and analyzed. Among 204 and 198 EGFP-LC3B punctate signals in WT cells and Drp1 KO cells, respectively, 43 and 37 signals disappeared before phagophore formation due to misfocusing of the microscope. The remaining 161 EGFP-LC3B signals were analyzed whether they were formed on fragment or tubular/clustered mitochondria and whether they became autophagosomes or mitophagosomes. (C) From the time-lapse imaging taken at 20-s intervals in WT and Drp1 KO cells, the length of time between the emergence of EGFP-LC3B signal on mitochondria and mitophagosome formation was measured. *n* = 10 in WT and 10 in Drp1 KO cells.

investigated mitochondrial morphology under the condition of mitophagy in the presence of bafilomycin A1. When *FIP200*, *ATG14*, or *WIPI2* was knocked down in WT and Drp1 KO cells, punctate mitochondria were barely observed (Fig. 9, A and B; and Fig. S3, E–I). In ATG5 or ATG3 knockdown cells, punctate mitochondria accumulated to a similar level as that in control siRNA cells (Fig. 9, A and B; and Fig. S3, E–I). The same results were obtained in FIP200 KO and ATG5 KO HeLa cells (Fig. 9 C). These findings strongly suggest that the factors required for nucleation and extension of isolation membranes, but not for the sealing of autophagosomes, are essential for mitochondrial division in mitophagy.

Because punctate mitochondria were not observed in FIP200, ATG14, and WIPI knockdown cells, even under the condition of mitophagy, isolation membrane formation and extension are likely to be essential for mitochondrial division in mitophagy. However, one possibility should be excluded before making a final conclusion. Mitochondrial division might occur before autophagosome formation to form punctate mitochondria, and the punctate mitochondria are sequestered and isolated

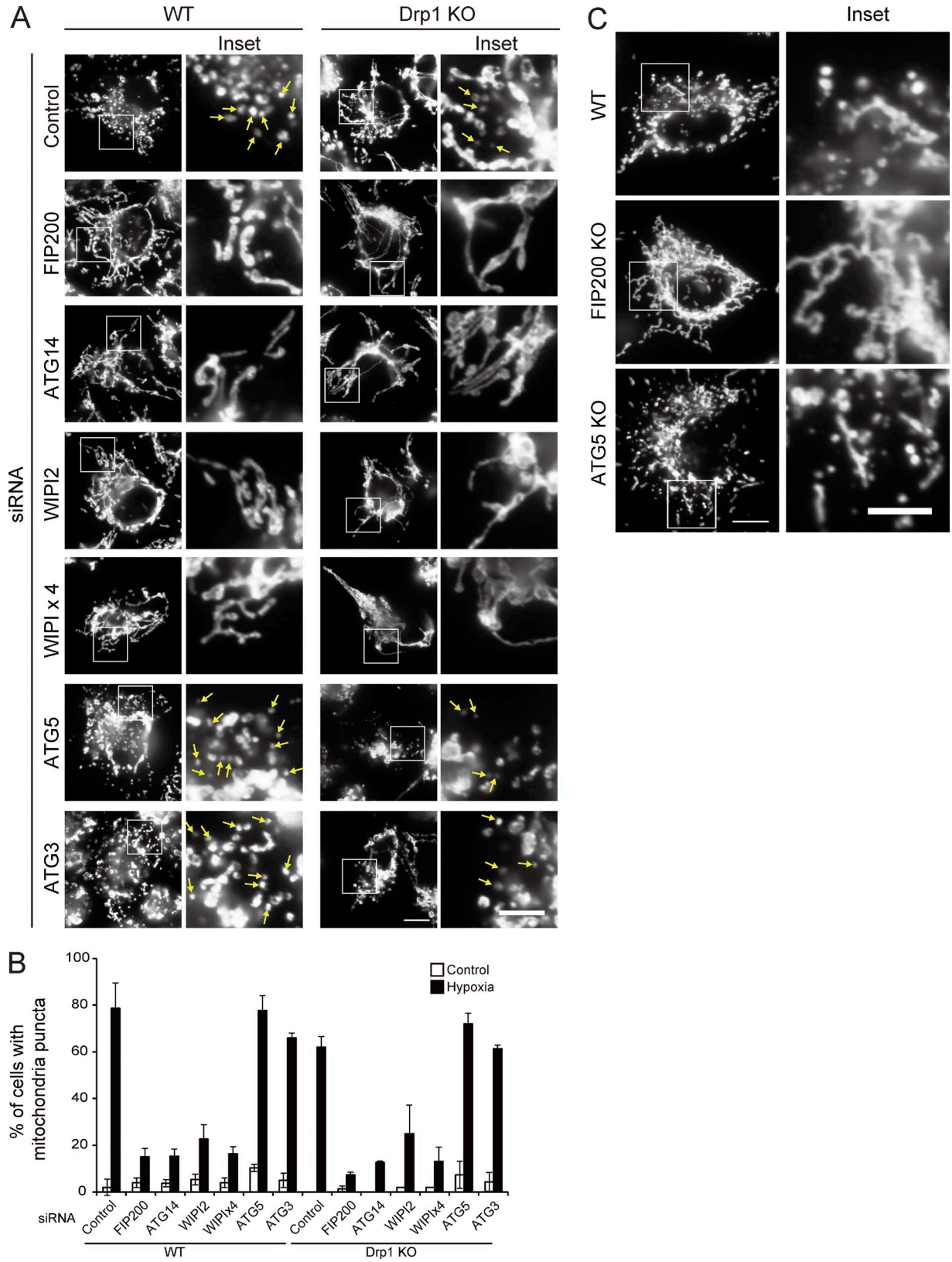

Figure 9. **Isolation membrane formation and extension are required for mitochondrial division upon induction of mitophagy.** (A and C) WT and Drp1 KO HeLa cells transfected with indicated siRNAs (A) or WT, FIP200 KO, and ATG5 KO HeLa cells (C) were cultured under hypoxic conditions for 24 h. The cells were treated with 100 nM bafilomycin A1 from 12 h after shifting to hypoxic conditions. After 24 h, the cells were examined by immunofluorescence microscopy with anti-Tom20 antibody. Small mitochondrial puncta are indicated by yellow arrows in insets. Bars: (main images) 10 µm; (insets) 5 µm. (B) Percentages of cells with small mitochondrial puncta were calculated from at least 50 cells under control and hypoxic conditions as shown in A. Data are shown as the mean ± SD of three independent experiments.

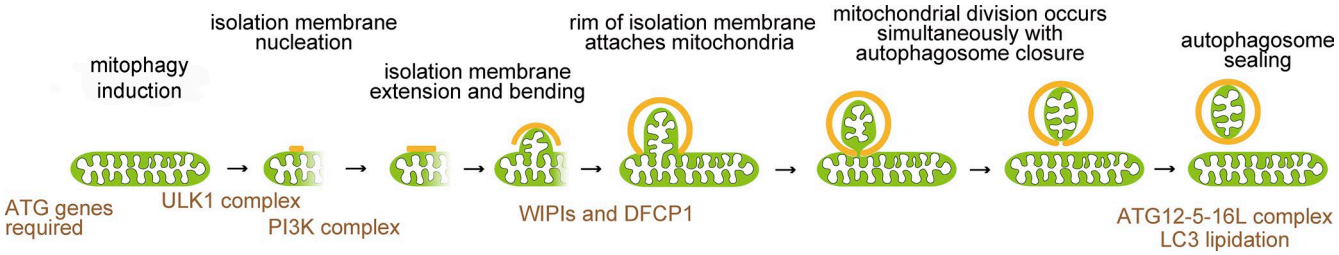

Figure 10. **Model of novel mitochondrial division involving autophagosome formation during mitophagy.**

by autophagosomes. However, in FIP200, ATG14, or WIPI knockdown cells, divided mitochondria might not be able to be isolated by autophagosomes. As a result, they might re-fuse with other mitochondria and form tubular or enlarged mitochondria (Figs. 9 and S5 B). This might be the reason that punctate mitochondria were not accumulated in FIP200, ATG14, or WIPI knockdown cells during the induction of mitophagy (Fig. 9). To exclude this possibility, we inhibited mitochondrial fusion by knockdown of MFN1/2 and investigated mitochondrial morphology (Fig. S5 C). In Drp1 KO and MFN1/2 knockdown cells, punctate mitochondria were accumulated in control, ATG5, and ATG3 knockdown cells, but not in FIP200, ATG14, and WIPI2 knockdown cells (Fig. S5, C and D). These results suggest that mitochondria undergo division only by extension of isolation membranes in Drp1 KO cells upon initiation of mitophagy.

Discussion

Mitophagy is thought to play an important role in mitochondrial quality control. Generally, mitochondrial division is believed to occur to isolate damaged parts of mitochondria from intact parts, and the damaged parts are then degraded by autophagy. This idea was initially proposed by Twig and Shirihai (Twig et al., 2008; Twig and Shirihai, 2011) and is now widely accepted. However, we propose here that the conventional model of mitochondrial division occurring before autophagosome formation is not common, or it is not the sole process of mitophagy.

In this study, we first investigated whether mitochondrial division factors are required for mitophagy. In budding yeast, deletion of Dnm1, which is a core machinery component for mitochondrial division, only partially reduced or delayed degradation of mitochondria by mitophagy compared with WT cells (Fig. 1, A–D). Interestingly, the diameter of mitochondria within the mitophagic bodies in *dnm1Δ* cells was ∼600 nm or less, which is almost the same size as those in WT cells, although all cytosolic mitochondria formed clustered spherical or long tubular structures (Figs. 1 F and S1 F). This finding suggests that mitochondria are divided into small punctate forms of ∼600 nm or less in diameter from parental clustered spherical or long tubular mitochondria in a Dnm1-independent manner. We next studied mammalian cells. As observed in yeast, in Drp1-defective mammalian cells, mitophagy was only partially reduced compared with WT cells (Figs. 2, 3, and S2). Interestingly, during mitophagy, nucleation of isolation membranes occurred on the mitochondria, and a small portion of mitochondria divided from a large mitochondrial mass simultaneously with isolation membrane extension. Isolation membranes are likely to induce mitochondrial bud formation and cleave the bud off from parental mitochondria (Fig. 7). This mitochondrial division during mitophagy is independent of Drp1 but is dependent on autophagosome formation machinery, such as FIP200, ATG14, and WIPIs (Figs. 8 A and 9). Taking all of these results into consideration, we conclude that mitochondria are divided in cooperation with isolation membrane formation and extension.

We propose the model of mitochondrial division for mitophagy (Fig. 10). When mitophagy is induced, isolation membranes emerge on the mitochondria and extend along the mitochondrial surface. In most cases, the mitochondrion makes a bud at the site of or close to isolation membrane formation, and then the isolation membrane starts enwrapping the budded portion of the mitochondrion. The budded portion of the mitochondrion is divided by an unidentified mechanism simultaneously with isolation membrane enclosure. Finally, complete sealing of the isolation membrane eventually occurs to form the mitophagosome. Based on this model, the size of enclosed mitochondria should be determined by the size of the autophagosome. Therefore, these models are consistent with the fact that similar sizes of mitochondria are always observed within vacuoles in yeast and are independent of the size and shape of cytosolic parental mitochondria (Figs. 1 F and S1, E and F).

We hypothesize two possibilities for the mitochondrial division mechanism at mitophagy. One possibility is that the mitochondrial bud is constricted and is directly divided by an extended isolation membrane. Based on physical analysis, an isolation membrane with a certain size and its partially bended form is energetically unstable and transforms to an energetically stable, almost closed form (this form still remains an unclosed hole; Knorr et al., 2012). This energetic difference between these two forms of isolation membranes might become the physical force for mitochondrial division upon mitophagy. Another possibility is that unidentified mitochondrial division machinery localizes and divides mitochondria at the site of isolation membrane closure. Further studies are required to clarify this issue.

In budding yeast, interaction of the mitochondrial outer membrane protein Atg32 and cytosolic adapter protein Atg11 is dispensable for the selection of mitochondria destined for degradation in mitophagy (Kanki et al., 2009c; Okamoto et al., 2009). Mao et al. (2013) reported that a division complex is recruited to degrade mitochondria through an interaction between Atg11 and Dnm1 and that this interaction is important for mitophagy. The authors showed that Atg11 recruits Dnm1 to the mitochondria and then mitochondrial division is performed after the induction of mitophagy. This finding is, in part, consistent with our result that mitochondrial division occurs simultaneously with the induction of mitophagy, but the importance of Dnm1 for mitophagy is different. Because deletion of *DNM1* partially reduced mitophagy in our study (Fig. 1 A), we also think that Dnm1 plays a role in mitophagy, but it is not an essential factor for mitophagy in yeast.

Although Drp1 was not involved in mitochondrial division for mitophagy, deletion of Drp1 slightly decreased mitophagy in mammalian cells (Figs. 2 E and S2 D). One of the possible reasons for this decrease in mitophagy is that Drp1 KO cells need a longer time to form mitophagosomes compared with WT cells (Fig. 8 C). It may be difficult to enwrap large clustered mitochondria in Drp1 KO cells by isolation membranes, and this difficulty may affect mitophagy in Drp1 KO cells.

Mitochondrial division by Dnm1/Drp1 is generally believed to be required for mitophagy and ensuring that the mitochondrial size is suitable for enwrapping by autophagosomes. However, the shape and size of mitochondria vary depending on cell types and culture conditions. Accordingly, a complicated mitochondrial division system/machinery is required to divide the variety of sizes and shapes of parental mitochondria into similar sizes of mitochondria for mitophagy. Therefore, this system may not always be efficient and stable. In this study, we propose a mitophagy process in which mitochondrial division occurs in synchronization with isolation membrane extension. This mitochondrial division does not require the canonical division factor Dnm1/Drp1, but needs the physical force of isolation membrane closure or unidentified division machinery. This model is reasonable because it enables enwrapping of the maximum size of mitochondria to fit into the autophagosome.

In this study, we mostly performed our experimental analyses under hypoxia or DFP-induced mitophagy conditions. However, other types of mitophagy have been reported, such as Parkin-mediated, starvation-induced, and induced pluripotent stem cell reprogramming–induced mitophagy (Narendra et al., 2008, 2010; Tanaka et al., 2010; Hirota et al., 2015; Ma et al., 2015). The role of Drp1 in these types of mitophagy remains unclear. Further studies are required to elucidate the roles of Drp1/Dnm1 in other types of mitophagy.

Materials and methods

Yeast strains and media

The yeast strains used in this study are shown in Tables S1 and S2. Yeast cells were grown in rich medium (YPD: 1% yeast extract, 2% peptone, and 2% glucose), lactate medium (YPL: 1% yeast extract, 2% peptone, and 2% lactate), or synthetic minimal medium with lactate (SML: 0.67% yeast nitrogen base, 2% lactate, and amino acids). Nitrogen starvation experiments were performed in synthetic minimal medium lacking nitrogen (SD-N: 0.17% yeast nitrogen base without amino acids and ammonium sulfate and 2% glucose). Cells were grown at 30°C.

Plasmids

The cDNAs encoding mito-Keima, mCherry, and BFP were amplified by PCR from pMT-mKeima-red (Medical and Biological Laboratories), pmCherry-C1 (Takara Bio Inc.), and pTagBFP-N (Evrogen), respectively. The cDNAs encoding LC3B, WIPI1, Drp1, Parkin, and LAMP1 were amplified by PCR from the cDNA pool. The PCR fragment of mito-Keima was ligated into pMXs-Puro (Cell Biolabs, Inc.) via the BamHI–EcoRI sites. *LC3B* was ligated into pMRX-IP (Saitoh et al., 2002) via the BamHI–NotI sites. To generate pMXs-Neo–mito-mCherry, a mito-mCherry fragment was amplified by PCR from the pMT-mCherry vector and ligated into pMXs-Neo (Cell Biolabs, Inc.) via the BamHI–EcoRI sites. To generate pMT-mCherry, the PCR fragment of mCherry from pmCherry-C1 was replaced with mKeima of pMT-mKeima-red by the PCR-based In-Fusion method (Takara Bio Inc.). For BFP-tagged constructs, BFP was ligated into NheI–BamHI sites of pcDNA3.1/Hygro(−) (Invitrogen), and then Drp1 and WIPI1 were cloned downstream and in-frame with BFP by the In-Fusion method. To generate LAMP1-EGFP, *LAMP1* and *EGFP* were ligated into the NheI–BamHI and BamHI–HindIII sites of pcDNA3.1/Hygro(−), respectively. Mff-IRES-GFP-NLS has been previously described (Otera et al., 2010). To generate Parkin-IRES-GFP-NLS, *Parkin* was replaced with *Mff* in Mff-IRES-GFP-NLS via the BamHI–NotI sites. To generate the mito-mCherry–EGFP-harboring tandem repeat mitochondrial targeting sequence (MTS), another MTS fragment and *EGFP* were inserted in-frame upstream and downstream of mCherry in pMT-mCherry, and then 2× MTS-mCherry–EGFP was ligated into the XhoI site of pCAGGS. To generate pRS416-RFP-Atg8, the RFP-Atg8 DNA fragment was digested from pRFP-Atg8 (414) (Legakis et al., 2007) via the BamHI–XhoI sites and ligated into the pRS416 vector (Sikorski and Hieter, 1989). To generate pBS-Puro, the PCR fragment of puromycin-resistant cassette from pTRE2puro vector (Takara Bio Inc.) was cloned into pBluescript SK(−) (Agilent Technologies).

Antibodies

Mouse monoclonal antibodies used in this study included anti-GFP (JL-8; Takara Bio Inc.), anti-ATG14 (4H8; Medical and Biological Laboratories), anti-ATG3 (3E8; Medical and Biological Laboratories), antimonomeric Keima-red (2F7; Medical and Biological Laboratories), anti-Drp1 (clone 8/DLP1; BD), anti-LC3 (clone LC3.1703; Cosmobio), anti-Mfn2 (XX-1; Santa Cruz Biotechnology, Inc.), anti-STX17 (2F8; Medical and Biological Laboratories), anti-Pgk1 (22C5; Molecular Probes), and anti-actin (MAB1501; EMD Millipore). Rabbit polyclonal antibodies that were used included anti-ATG5 (PM050; Medical and Biological Laboratories), anti-Mfn1 (H-65; Santa Cruz Biotechnology, Inc.), and anti-Tom20 (F-145; Santa Cruz Biotechnology, Inc.). Anti-FIP200 rabbit monoclonal antibody (D10D11; Cell Signaling Technology) was used.

Mitophagy assays

To monitor mitophagy in *S. cerevisiae* and *P. pastoris*, the Idh1-GFP processing assay was performed as previously described (Kanki et al., 2009a; Aihara et al., 2014). For mammalian mitophagy, the mito-Keima assay was performed as previously described (Hirota et al., 2015). The level of mitophagy can be estimated by counting the number of punctate structures observed when excited by 590-nm light using Metamorph 7 software (Molecular Devices).

Fluorescence microscopy of yeast

Fluorescence microscopy was performed using a microscope (IX73; Olympus) with a UPlanSApo 100× oil objective lens (NA of 1.40) and a cooled charge-coupled device camera (EXi Blue; QImaging). The mutant cells expressing Idh1-GFP, Om45-GFP, or RFP-Atg8 were cultured in YPL medium until the mid-log growth phase and then shifted to SD-N medium for 6 h. 3D fluorescence images of cells were acquired with a 0.1-µm z axis step size. The images were analyzed by the 3D deconvolution module of Metamorph 7 software.

EM

The *pep4Δ* and *pep4Δ/dnm1Δ* strains were cultured in YPL medium to mid-log phase and then shifted to SD-N and cultured for 6 h. Cells were pelleted and cryoimmobilized by high-pressure freezing using a high-pressure freezing system (EM ICE; Leica Biosystems). All samples were freeze substituted and embedded to Lowicryl (Electron Microscopy Sciences) using a temperature-controlled device (AFS2; Leica Biosystems) as previously described (Hasegawa et al., 2016). 60-nm sections were cut with a microtome and stained with lead citrate and then observed using a

transmission electron microscope (1011; JEOL). For chemical fixation of yeast, cells were fixed and embedded according to previously described procedures (Wright, 2000). For mammalian cells, cells were cultured as described in morphological analysis and then fixed with 2% glutaraldehyde and 2% paraformaldehyde in 0.1 M phosphate buffer, pH 7.4, for 10 min at room temperature and then for 50 min at 4°C. The cells were washed three times for 10 min with 0.1 M phosphate buffer, pH 7.4, and then postfixed with 1% osmium tetroxide in 0.1 M phosphate buffer, pH 7.4, for 60 min at 4°C. The cells were dehydrated with ethanol and embedded in EPON812. Ultrathin sections were observed using an electron microscope (H-7650; Hitachi).

Mammalian cell culture, induction of mitophagy, and DNA transfection

HeLa cells, SH-SY5Y cells, and MEFs were cultured with DMEM supplemented with 10% FBS and maintained at 37°C under 5% CO_2. This was defined as the control culture condition in this study. For hypoxia-induced mitophagy, the cells were cultured with normal medium under hypoxic conditions (1% O_2, 94% N_2, and 5% CO_2) using a multigas incubator (APM-30D; Astec Corporation). For DFP-induced mitophagy, cells were cultured with normal medium supplemented with 1 mM DFP (Wako Pure Chemical Industries) under normal conditions. For Parkin-dependent mitophagy, cells were transfected with Parkin-IRES-GFP-NLS and cultured for 24 h and then cultured for an additional 6 h with 10 µM CCCP (Wako Pure Chemical Industries). DNA transfection was performed using FuGENE HD (Promega) according to the manufacturer's instructions.

siRNA-mediated knockdown

We performed siRNA-mediated knockdown in HeLa cells and SH-SY5Y cells. In brief, siRNAs were transfected into cells using Lipofectamine 2000 (Invitrogen) according to the manufacturer's instructions. After 2 d, the cells were detached from dishes using trypsin-EDTA and resuspended with DMEM with FBS and the same siRNA. The cells were cultured for an additional 2 d and then shifted to mitophagy conditions. We used the following sequences of siRNAs: human Drp1 siRNA sense, 5′-GUAAUACUGAGACUUUGUUTT-3′, and antisense, 5′-AACAAAGUCUCAGUAUUACTT-3′; human MFN1 siRNA sense, 5′-CUUCCUAAGUGUUGAAGGATT-3′, and antisense, 5′-UCCUUCAACACUUAGGAAGTT-3′; human MFN2 siRNA sense, 5′-GUGAUGUGGCCCAACUCUATT-3′, and antisense, 5′-UAGAGUUGGGCCACAUCACTT-3′; human FIP200 siRNA sense, 5′-GAUCUUAUGUAGUCGUCCATT-3′, and antisense, 5′-UGGACGAUCACAUAAGAUCTT-3′; human ATG14 siRNA sense, 5′-GCAAGAUGAGGAUUGAACATT-3′, and antisense, 5′-UGUUCAAUCCUCAUCUUGCTT-3′; human WIPI1 siRNA sense, 5′-GUCUAUGUGCUCUCUCUAUTT-3′, and antisense, 5′-AUAGAGAGAGCACAUAGACTT-3′; human WIPI2 siRNA sense, 5′-GACAUGAAGGUGCUGCAUATT-3′, and antisense, 5′-UAUGCAGCACCUUCAUGUCTT-3′; human WDR45L siRNA sense, 5′-CCAAUAUUUACUGCAUCAATT-3′, and antisense, 5′-UUGAUGCAGUAAAUAUUGGTT-3′; human WDR45 siRNA sense, 5′-GUCCAUAUCUUUGCUCUCATT-3′, and antisense, 5′-UGAGAGCAAAGAUAUGGACTT-3′; human ATG5 siRNA sense, 5′-CAGCAUACAAUCUCAGAAA-3′, and antisense, 5′-UUUCUGAGAUUGUAUGCUG-3′; human ATG3 siRNA sense, 5′-CAUUGAGACUGUUGCAGAATT-3′, and antisense, 5′-UUCUGCAACAGUCUCAAUGTT-3′; human STX17 siRNA sense, 5′-CUGAAAUUCCUCAAGAUCATT-3′, and antisense 5′-UGAUCUUGAGGAAUUUCAGTT-3′; and luciferase siRNA sense, 5′-UUCACUGGCGACGUAAUCCACGAUC-3′, and antisense, 5′-GAUCGUGGAUUACGUCGCCAGUGAA-3′.

Generation of KO HeLa cells using the CRISPR-Cas9 system

To generate several gene KO HeLa cells, we used the CRISPR-Cas9 system (Cong et al., 2013). Drp1 KO, Mff KO, Fis1 KO, and MiD49/51 double KOs were generated as previously described (Otera et al., 2016). For FIP200 and ATG5 KO HeLa cells, guide RNAs were selected from FIP200 exon 4 (5′-CACCAGGTGCTGGTGGTCAATGG-3′) and ATG5 exon 2 (5′-AAGATGTGCTTCGAGATGTGTGG-3′) and were ligated into pX330-U6-Chimeric_BB-CBh-hSpCas9 (42230; Addgene), a gift from F. Zhang (Massachusetts Institute of Technology, Cambridge, MA). These CRISPR plasmids were cotransfected with pBS-Puro into WT HeLa cells. 1 d after transfection, the transfected cells were enriched with puromycin-containing medium for several days and then cloned by limiting dilution in 96-well plates with normal medium. The KO cell lines were verified by immunoblot analysis with anti-FIP200 or anti-ATG5 antibodies and DNA sequence analysis of the target regions.

Generation of stable cell lines using a retroviral infection system

To generate stable cell lines expressing mito-Keima or coexpressing mito-mCherry and EGFP-LC3B, we used a retroviral infection system with several retroviral vectors, described as follows. HeLa cells and SH-SY5Y cells were transiently transfected with mouse cationic amino acid transporter 1 for presenting the ecotropic retroviral receptor on the cell surface. These transfected cells were then incubated with retrovirus-containing medium with 8 µg/ml polybrene for 24 h. MEFs were directly incubated with retrovirus. The infected stable cell lines were selected with medium containing puromycin or G418. To produce the retroviruses, Plat-E cells (Cell Biolabs, Inc.) were transfected with retroviral vectors expressing mito-Keima, mito-mCherry, or EGFP-LC3B using FuGENE HD (Promega) according to the manufacturer's instructions. 2 d after transfection, culture medium containing retrovirus was harvested and filtered.

Morphological analysis

Cells were cultured on coverslips overnight and then shifted to mitophagy conditions in the presence of bafilomycin A1. After induction of mitophagy, cells were fixed with 4% paraformaldehyde for 15 min at room temperature. Fixed cells were permeabilized with 50 µg/ml digitonin/PBS for 5 min and then blocked with 1% bovine serum albumin/PBS for 30 min. Immunofluorescence staining was performed with primary antibodies against LC3 and Tom20 and secondary antibodies conjugated with Alexa Fluor 488 and 594. Cells were monitored by an IX73 microscope with a UPlanSApo 100× oil objective lens (NA of 1.40). Percentages of cells with small mitochondrial puncta were quantified from at least 50 cells using a cell count program of ImageJ software (National Institutes of Health). All data are shown as the mean ± SD of three independent experiments.

Live-cell imaging

Live-cell imaging was performed using an IX73 microscope with a UPlanSApo 100× oil objective lens (NA of 1.40) and a cooled charge-coupled device camera. The cells were maintained by a stage-top incubator (TOKAI HIT) at 37°C under 5% CO_2 during investigation. The cells were precultured on a glass-bottomed dish overnight, and then the medium was replaced with mitophagy medium containing 1 mM DFP. After 12 h, the dish was transferred to the stage and examined. Time-lapse images were acquired at 20-s intervals and processed by Metamorph 7.

Online supplemental material

Fig. S1 shows that Dnm1-independent mitochondrial division occurs during mitophagy in yeast. Fig. S2 shows that hypoxia-induced and DFP-induced mitophagy can be observed by tandem fluorescent protein

reporter and immunoblot analysis in Drp1 KO HeLa cells. Fig. S3 shows that mitochondrial fragmentation does not enhance mitophagy flux and Drp1 is dispensable for Parkin-mediated mitophagy. Fig. S4 shows that Drp1-independent mitochondrial fragmentation appears under the condition of mitophagy in HeLa cells and isolation membranes emerge on tubular mitochondria. Fig. S5 shows that Drp1-independent mitochondrial division in mitophagy requires isolation membrane extension, even in MFN knockdown cells. Table S1 is a list of *S. cerevisiae* strains used in this study. Table S2 is a list of *P. pastris* strains used in this study.

Acknowledgments

We thank Daniel J. Klionsky (University of Michigan, Ann Arbor, MI), Shoji Yamaoka (Tokyo Medical and Dental University, Tokyo, Japan), and Feng Zhang for providing plasmids and Hiroyuki Katayama and Atsushi Miyawaki for helping with the Keima experiments. We also thank Satoshi Waguri for helping with EM.

This work was supported in part by the Ministry of Education, Culture, Sports, Science and Technology program "Promotion of Environmental Improvement for Independence of Young Researchers" under the Special Coordination Funds for Promoting Science and Technology (to T. Kanki); the Japan Society for the Promotion of Science KAKENHI grants 26291039 (to T. Kanki), 16H01384 (to T. Kanki), 16H01198 (to T. Kanki), 15K18501 (to S.-i. Yamashita), and 16K18514 (to K. Furukawa); the Yujin Memorial grant (Niigata University School of Medicine; to T. Kanki); The Sumitomo Foundation (to T. Kanki); the Astellas Foundation for Research on Metabolic Disorders (to T. Kanki); and the Takeda Science Foundation (to S.-i. Yamashita and T. Kanki).

The authors declare no competing financial interests.

Submitted: 24 May 2016
Revised: 2 September 2016
Accepted: 26 October 2016

References

Abeliovich, H., M. Zarei, K.T. Rigbolt, R.J. Youle, and J. Dengjel. 2013. Involvement of mitochondrial dynamics in the segregation of mitochondrial matrix proteins during stationary phase mitophagy. *Nat. Commun.* 4:2789. http://dx.doi.org/10.1038/ncomms3789

Aihara, M., X. Jin, Y. Kurihara, Y. Yoshida, Y. Matsushima, M. Oku, Y. Hirota, T. Saigusa, Y. Aoki, T. Uchiumi, et al. 2014. Tor and the Sin3-Rpd3 complex regulate expression of the mitophagy receptor protein Atg32 in yeast. *J. Cell Sci.* 127:3184–3196. http://dx.doi.org/10.1242/jcs.153254

Allen, G.F., R. Toth, J. James, and I.G. Ganley. 2013. Loss of iron triggers PINK1/Parkin-independent mitophagy. *EMBO Rep.* 14:1127–1135. http://dx.doi.org/10.1038/embor.2013.168

Arasaki, K., H. Shimizu, H. Mogari, N. Nishida, N. Hirota, A. Furuno, Y. Kudo, M. Baba, N. Baba, J. Cheng, et al. 2015. A role for the ancient SNARE syntaxin 17 in regulating mitochondrial division. *Dev. Cell.* 32:304–317. http://dx.doi.org/10.1016/j.devcel.2014.12.011

Bernhardt, D., M. Müller, A.S. Reichert, and H.D. Osiewacz. 2015. Simultaneous impairment of mitochondrial fission and fusion reduces mitophagy and shortens replicative lifespan. *Sci. Rep.* 5:7885. http://dx.doi.org/10.1038/srep07885

Cong, L., F.A. Ran, D. Cox, S. Lin, R. Barretto, N. Habib, P.D. Hsu, X. Wu, W. Jiang, L.A. Marraffini, and F. Zhang. 2013. Multiplex genome engineering using CRISPR/Cas systems. *Science.* 339:819–823. http://dx.doi.org/10.1126/science.1231143

Detmer, S.A., and D.C. Chan. 2007. Functions and dysfunctions of mitochondrial dynamics. *Nat. Rev. Mol. Cell Biol.* 8:870–879. http://dx.doi.org/10.1038/nrm2275

Geisler, S., K.M. Holmström, D. Skujat, F.C. Fiesel, O.C. Rothfuss, P.J. Kahle, and W. Springer. 2010. PINK1/Parkin-mediated mitophagy is dependent on VDAC1 and p62/SQSTM1. *Nat. Cell Biol.* 12:119–131. http://dx.doi.org/10.1038/ncb2012

Griparic, L., and A.M. van der Bliek. 2001. The many shapes of mitochondrial membranes. *Traffic.* 2:235–244. http://dx.doi.org/10.1034/j.1600-0854.2001.1r008.x

Hamasaki, M., N. Furuta, A. Matsuda, A. Nezu, A. Yamamoto, N. Fujita, H. Oomori, T. Noda, T. Haraguchi, Y. Hiraoka, et al. 2013. Autophagosomes form at ER-mitochondria contact sites. *Nature.* 495:389–393. http://dx.doi.org/10.1038/nature11910

Hasegawa, J., R. Iwamoto, T. Otomo, A. Nezu, M. Hamasaki, and T. Yoshimori. 2016. Autophagosome-lysosome fusion in neurons requires INPP5E, a protein associated with Joubert syndrome. *EMBO J.* 35:1853–1867. http://dx.doi.org/10.15252/embj.201593148

Hirota, Y., S. Yamashita, Y. Kurihara, X. Jin, M. Aihara, T. Saigusa, D. Kang, and T. Kanki. 2015. Mitophagy is primarily due to alternative autophagy and requires the MAPK1 and MAPK14 signaling pathways. *Autophagy.* 11:332–343. http://dx.doi.org/10.1080/15548627.2015.1023047

Ikeda, Y., A. Shirakabe, Y. Maejima, P. Zhai, S. Sciarretta, J. Toli, M. Nomura, K. Mihara, K. Egashira, M. Ohishi, et al. 2015. Endogenous Drp1 mediates mitochondrial autophagy and protects the heart against energy stress. *Circ. Res.* 116:264–278. http://dx.doi.org/10.1161/CIRCRESAHA.116.303356

Ishihara, N., M. Nomura, A. Jofuku, H. Kato, S.O. Suzuki, K. Masuda, H. Otera, Y. Nakanishi, I. Nonaka, Y. Goto, et al. 2009. Mitochondrial fission factor Drp1 is essential for embryonic development and synapse formation in mice. *Nat. Cell Biol.* 11:958–966. http://dx.doi.org/10.1038/ncb1907

Itakura, E., C. Kishi-Itakura, and N. Mizushima. 2012. The hairpin-type tail-anchored SNARE syntaxin 17 targets to autophagosomes for fusion with endosomes/lysosomes. *Cell.* 151:1256–1269. http://dx.doi.org/10.1016/j.cell.2012.11.001

Kageyama, Y., M. Hoshijima, K. Seo, D. Bedja, P. Sysa-Shah, S.A. Andrabi, W. Chen, A. Höke, V.L. Dawson, T.M. Dawson, et al. 2014. Parkin-independent mitophagy requires Drp1 and maintains the integrity of mammalian heart and brain. *EMBO J.* 33:2798–2813. http://dx.doi.org/10.15252/embj.201488658

Kanki, T., and D.J. Klionsky. 2008. Mitophagy in yeast occurs through a selective mechanism. *J. Biol. Chem.* 283:32386–32393. http://dx.doi.org/10.1074/jbc.M802403200

Kanki, T., D. Kang, and D.J. Klionsky. 2009a. Monitoring mitophagy in yeast: the Om45-GFP processing assay. *Autophagy.* 5:1186–1189. http://dx.doi.org/10.4161/auto.5.8.9854

Kanki, T., K. Wang, M. Baba, C.R. Bartholomew, M.A. Lynch-Day, Z. Du, J. Geng, K. Mao, Z. Yang, W.L. Yen, and D.J. Klionsky. 2009b. A genomic screen for yeast mutants defective in selective mitochondria autophagy. *Mol. Biol. Cell.* 20:4730–4738. http://dx.doi.org/10.1091/mbc.E09-03-0225

Kanki, T., K. Wang, Y. Cao, M. Baba, and D.J. Klionsky. 2009c. Atg32 is a mitochondrial protein that confers selectivity during mitophagy. *Dev. Cell.* 17:98–109. http://dx.doi.org/10.1016/j.devcel.2009.06.014

Katayama, H., T. Kogure, N. Mizushima, T. Yoshimori, and A. Miyawaki. 2011. A sensitive and quantitative technique for detecting autophagic events based on lysosomal delivery. *Chem. Biol.* 18:1042–1052. http://dx.doi.org/10.1016/j.chembiol.2011.05.013

Kirisako, T., M. Baba, N. Ishihara, K. Miyazawa, M. Ohsumi, T. Yoshimori, T. Noda, and Y. Ohsumi. 1999. Formation process of autophagosome is traced with Apg8/Aut7p in yeast. *J. Cell Biol.* 147:435–446. http://dx.doi.org/10.1083/jcb.147.2.435

Kishi-Itakura, C., I. Koyama-Honda, E. Itakura, and N. Mizushima. 2014. Ultrastructural analysis of autophagosome organization using mammalian autophagy-deficient cells. *J. Cell Sci.* 127:4089–4102. http://dx.doi.org/10.1242/jcs.156034

Klionsky, D.J., Z. Elazar, P.O. Seglen, and D.C. Rubinsztein. 2008. Does bafilomycin A_1 block the fusion of autophagosomes with lysosomes? *Autophagy.* 4:849–850. http://dx.doi.org/10.4161/auto.6845

Knorr, R.L., R. Dimova, and R. Lipowsky. 2012. Curvature of double-membrane organelles generated by changes in membrane size and composition. *PLoS One.* 7:e32753. http://dx.doi.org/10.1371/journal.pone.0032753

Lazarou, M., D.A. Sliter, L.A. Kane, S.A. Sarraf, C. Wang, J.L. Burman, D.P. Sideris, A.I. Fogel, and R.J. Youle. 2015. The ubiquitin kinase PINK1 recruits autophagy receptors to induce mitophagy. *Nature.* 524:309–314. http://dx.doi.org/10.1038/nature14893

Legakis, J.E., W.L. Yen, and D.J. Klionsky. 2007. A cycling protein complex required for selective autophagy. *Autophagy.* 3:422–432. http://dx.doi.org/10.4161/auto.4129

Lemasters, J.J. 2005. Selective mitochondrial autophagy, or mitophagy, as a targeted defense against oxidative stress, mitochondrial dysfunction, and aging. *Rejuvenation Res.* 8:3–5. http://dx.doi.org/10.1089/rej.2005.8.3

Levine, B., N. Mizushima, and H.W. Virgin. 2011. Autophagy in immunity and inflammation. *Nature.* 469:323–335. http://dx.doi.org/10.1038/nature09782

Liu, L., D. Feng, G. Chen, M. Chen, Q. Zheng, P. Song, Q. Ma, C. Zhu, R. Wang, W. Qi, et al. 2012. Mitochondrial outer-membrane protein FUNDC1 mediates hypoxia-induced mitophagy in mammalian cells. *Nat. Cell Biol.* 14:177–185. http://dx.doi.org/10.1038/ncb2422

Ma, T., J. Li, Y. Xu, C. Yu, T. Xu, H. Wang, K. Liu, N. Cao, B.M. Nie, S.Y. Zhu, et al. 2015. Atg5-independent autophagy regulates mitochondrial clearance and is essential for iPSC reprogramming. *Nat. Cell Biol.* 17:1379–1387. http://dx.doi.org/10.1038/ncb3256

Mao, K., K. Wang, X. Liu, and D.J. Klionsky. 2013. The scaffold protein Atg11 recruits fission machinery to drive selective mitochondria degradation by autophagy. *Dev. Cell.* 26:9–18. http://dx.doi.org/10.1016/j.devcel.2013.05.024

Mendl, N., A. Occhipinti, M. Müller, P. Wild, I. Dikic, and A.S. Reichert. 2011. Mitophagy in yeast is independent of mitochondrial fission and requires the stress response gene *WHI2*. *J. Cell Sci.* 124:1339–1350. http://dx.doi.org/10.1242/jcs.076406

Mizushima, N., Y. Ohsumi, and T. Yoshimori. 2002. Autophagosome formation in mammalian cells. *Cell Struct. Funct.* 27:421–429. http://dx.doi.org/10.1247/csf.27.421

Nakatogawa, H., K. Suzuki, Y. Kamada, and Y. Ohsumi. 2009. Dynamics and diversity in autophagy mechanisms: lessons from yeast. *Nat. Rev. Mol. Cell Biol.* 10:458–467. http://dx.doi.org/10.1038/nrm2708

Narendra, D., A. Tanaka, D.F. Suen, and R.J. Youle. 2008. Parkin is recruited selectively to impaired mitochondria and promotes their autophagy. *J. Cell Biol.* 183:795–803. http://dx.doi.org/10.1083/jcb.200809125

Narendra, D.P., S.M. Jin, A. Tanaka, D.F. Suen, C.A. Gautier, J. Shen, M.R. Cookson, and R.J. Youle. 2010. PINK1 is selectively stabilized on impaired mitochondria to activate Parkin. *PLoS Biol.* 8:e1000298. http://dx.doi.org/10.1371/journal.pbio.1000298

Nixon, R.A. 2013. The role of autophagy in neurodegenerative disease. *Nat. Med.* 19:983–997. http://dx.doi.org/10.1038/nm.3232

Okamoto, K., N. Kondo-Okamoto, and Y. Ohsumi. 2009. Mitochondria-anchored receptor Atg32 mediates degradation of mitochondria via selective autophagy. *Dev. Cell.* 17:87–97. http://dx.doi.org/10.1016/j.devcel.2009.06.013

Otera, H., C. Wang, M.M. Cleland, K. Setoguchi, S. Yokota, R.J. Youle, and K. Mihara. 2010. Mff is an essential factor for mitochondrial recruitment of Drp1 during mitochondrial fission in mammalian cells. *J. Cell Biol.* 191:1141–1158. http://dx.doi.org/10.1083/jcb.201007152

Otera, H., N. Ishihara, and K. Mihara. 2013. New insights into the function and regulation of mitochondrial fission. *Biochim. Biophys. Acta.* 1833:1256–1268. http://dx.doi.org/10.1016/j.bbamcr.2013.02.002

Otera, H., N. Miyata, O. Kuge, and K. Mihara. 2016. Drp1-dependent mitochondrial fission via MiD49/51 is essential for apoptotic cristae remodeling. *J. Cell Biol.* 212:531–544. http://dx.doi.org/10.1083/jcb.201508099

Proikas-Cezanne, T., S. Ruckerbauer, Y.D. Stierhof, C. Berg, and A. Nordheim. 2007. Human WIPI-1 puncta-formation: a novel assay to assess mammalian autophagy. *FEBS Lett.* 581:3396–3404. http://dx.doi.org/10.1016/j.febslet.2007.06.040

Rambold, A.S., B. Kostelecky, N. Elia, and J. Lippincott-Schwartz. 2011. Tubular network formation protects mitochondria from autophagosomal degradation during nutrient starvation. *Proc. Natl. Acad. Sci. USA.* 108:10190–10195. http://dx.doi.org/10.1073/pnas.1107402108

Saitoh, T., H. Nakano, N. Yamamoto, and S. Yamaoka. 2002. Lymphotoxin-β receptor mediates NEMO-independent NF-kappaB activation. *FEBS Lett.* 532:45–51. http://dx.doi.org/10.1016/S0014-5793(02)03622-0

Sakai, Y., A. Koller, L.K. Rangell, G.A. Keller, and S. Subramani. 1998. Peroxisome degradation by microautophagy in *Pichia pastoris*: identification of specific steps and morphological intermediates. *J. Cell Biol.* 141:625–636. http://dx.doi.org/10.1083/jcb.141.3.625

Sikorski, R.S., and P. Hieter. 1989. A system of shuttle vectors and yeast host strains designed for efficient manipulation of DNA in *Saccharomyces cerevisiae*. *Genetics.* 122:19–27.

Smirnova, E., L. Griparic, D.L. Shurland, and A.M. van der Bliek. 2001. Dynamin-related protein Drp1 is required for mitochondrial division in mammalian cells. *Mol. Biol. Cell.* 12:2245–2256. http://dx.doi.org/10.1091/mbc.12.8.2245

Song, M., K. Mihara, Y. Chen, L. Scorrano, and G.W. Dorn II. 2015. Mitochondrial fission and fusion factors reciprocally orchestrate mitophagic culling in mouse hearts and cultured fibroblasts. *Cell Metab.* 21:273–285. http://dx.doi.org/10.1016/j.cmet.2014.12.011

Sou, Y.S., S. Waguri, J. Iwata, T. Ueno, T. Fujimura, T. Hara, N. Sawada, A. Yamada, N. Mizushima, Y. Uchiyama, et al. 2008. The Atg8 conjugation system is indispensable for proper development of autophagic isolation membranes in mice. *Mol. Biol. Cell.* 19:4762–4775. http://dx.doi.org/10.1091/mbc.E08-03-0309

Takeshige, K., M. Baba, S. Tsuboi, T. Noda, and Y. Ohsumi. 1992. Autophagy in yeast demonstrated with proteinase-deficient mutants and conditions for its induction. *J. Cell Biol.* 119:301–311. http://dx.doi.org/10.1083/jcb.119.2.301

Tanaka, A., M.M. Cleland, S. Xu, D.P. Narendra, D.F. Suen, M. Karbowski, and R.J. Youle. 2010. Proteasome and p97 mediate mitophagy and degradation of mitofusins induced by Parkin. *J. Cell Biol.* 191:1367–1380. http://dx.doi.org/10.1083/jcb.201007013

Twig, G., and O.S. Shirihai. 2011. The interplay between mitochondrial dynamics and mitophagy. *Antioxid. Redox Signal.* 14:1939–1951. http://dx.doi.org/10.1089/ars.2010.3779

Twig, G., A. Elorza, A.J. Molina, H. Mohamed, J.D. Wikstrom, G. Walzer, L. Stiles, S.E. Haigh, S. Katz, G. Las, et al. 2008. Fission and selective fusion govern mitochondrial segregation and elimination by autophagy. *EMBO J.* 27:433–446. http://dx.doi.org/10.1038/sj.emboj.7601963

Wright, R. 2000. Transmission electron microscopy of yeast. *Microsc. Res. Tech.* 51:496–510. http://dx.doi.org/10.1002/1097-0029(20001215)51:6<496::AID-JEMT2>3.0.CO;2-9